

LINEAR OPTIMAL STABILIZATION AND REPRESENTATION
OF MULTI-MACHINE POWER SYSTEMS

by

HAMDY ALY MOHAMMED MOUSSA

B.Sc., Ain Shams University, Egypt, 1965

M.Sc., Ain Shams University, Egypt, 1969

A THESIS SUBMITTED IN PARTIAL FULFILMENT OF
THE REQUIREMENTS FOR THE DEGREE OF

DOCTOR OF PHILOSOPHY

in the Department of
Electrical Engineering

We accept this thesis as conforming to the
required standard

Research Supervisor.....

Members of the Committee.....

.....

.....

Head of the Department.....

Members of the Department
of Electrical Engineering

THE UNIVERSITY OF BRITISH COLUMBIA

July, 1971

In presenting this thesis in partial fulfilment of the requirements for an advanced degree at the University of British Columbia, I agree that the Library shall make it freely available for reference and study. I further agree that permission for extensive copying of this thesis for scholarly purposes may be granted by the Head of my Department or by his representatives. It is understood that copying or publication of this thesis for financial gain shall not be allowed without my written permission.

Department of Electrical Engineering

The University of British Columbia
Vancouver 8, Canada

Date August 3, 1971

ABSTRACT

Linear optimal regulators have been designed for power system stabilization by introducing control signals to voltage regulators and/or governors. A new technique is developed in this thesis to determine the state weighting matrix Q of the regulator performance function with a dominant eigenvalue shift of the closed loop optimal system. The technique is used to investigate the stabilization of a typical one-machine infinite system and a multi-machine system with different stabilization schemes. The objective is to find the best way to stabilize a power system. An optimally sensitive controller is also developed to offset the effects of the changing system operating conditions on the effort of the stabilizing signal. The controller automatically adjusts its gains so that it always provides the system with the optimum stabilizing signal. A new multi-machine state variable formulation, necessary for these studies, is developed. It requires minimum computations and retains all the parameter information for sensitivity studies. An exact representation of synchronous machines is investigated and test methods are suggested for the determination of exact circuit parameters.

TABLE OF CONTENTS

	Page
ABSTRACT.....	ii
TABLE OF CONTENTS.....	iii
LIST OF TABLES.....	vi
LIST OF ILLUSTRATIONS.....	vii
ACKNOWLEDGMENT.....	viii
NOMENCLATURE.....	ix
1. INTRODUCTION.....	1
2. EXACT EQUIVALENT CIRCUITS AND PARAMETERS OF SYNCHRONOUS MACHINES....	4
2.1. d-Axis Exact Equivalent Circuits.....	4
2.2. q-Axis Exact Equivalent Circuits.....	8
2.3. Circuit Parameters in Terms of Conventional Parameters.....	11
2.4. Extra Tests to Determine T_D and x''_{do}	13
2.4.1. Determination of T_D From a Varying Slip Test.....	13
2.4.2. Determination of T_D From Decaying Current Test.....	14
2.4.3. Determination of x''_{do}	16
2.5. Laboratory Test Results.....	17
3. STATE VARIABLE EQUATIONS OF MULTI-MACHINE POWER SYSTEMS.....	19
3.1. Terminal Voltages and Currents.....	19
3.2. Nonlinear Machine Equations.....	21
3.3. Linearized Machine Equations.....	23
3.4. Exciter and Voltage Regulator System.....	25
3.5. Torque Equations.....	26
3.6. Governor-hydraulic System.....	28

	Page
3.7. State Equations.....	29
3.8. Multi-machine System with an Infinite Bus.....	29
3.9. Simplification of Power System Dynamics.....	31
4. OPTIMAL LINEAR REGULATOR DESIGN WITH DOMINANT EIGENVALUE SHIFT.....	34
4.1. Linear Optimal Regulator Problem.....	34
4.2. Eigenvalue Shift Policy.....	35
4.3. The Shift.....	36
4.4. Determination of Δq	37
4.5. Sensitivity Coefficients λ, q	37
4.6. Algorithm.....	40
5. OPTIMAL POWER SYSTEM STABILIZATION THROUGH EXCITATION AND/OR GOVERNOR CONTROL.....	41
5.1. System Data.....	41
5.2. Case 1: u_E Control.....	43
5.3. Case 2a: u_G Control, with Dashpot.....	44
5.4. Case 2b: u'_G Control, without Dashpot.....	45
5.5. Case 3: u_E Plus u'_G Control.....	46
5.6. Nonlinear Tests.....	47
6. OPTIMAL STABILIZATION OF A MULTI-MACHINE SYSTEM.....	51
6.1. System Data and Description.....	51
6.2. Case 1: One Machine Optimal Excitation Control u_{EI}	54
6.3. Case 2: Multi-Optimal Controllers u_{EM}	55
6.4. Case 3: Approximated One Machine Optimal Design.....	57
6.5. Case 4: Subsystems Optimal Design.....	58

	Page
6.6. Nonlinear Tests.....	59
7. OPTIMUM STABILIZATION OF POWER SYSTEMS OVER WIDE RANGE OPERATING CONDITIONS.....	63
7.1. Optimally Sensitive Linear Regulator Design.....	63
7.2. Sensitivity Equations of the Linearized Power System.....	66
7.3. Optimally Sensitive Stabilization of a Power System.....	71
8. CONCLUSIONS.....	81
APPENDIX A.....	84
APPENDIX B.....	86
REFERENCES.....	90

LIST OF TABLES

TABLE		PAGE
3-1	Eigenvalues of the Typical One Machine Infinite System of Different Modelling.....	33
7-1	Controller Gains for u_{ES} and u_E^* at Different Operating Conditions.....	77
7-2	Dominant Eigenvalues of the System with the Different Controllers.....	78

LIST OF ILLUSTRATIONS

FIGURE		PAGE
2-1	General d-Axis Circuits.....	7
2-2	Simplified d-Axis Circuit.....	7
2-3	General q-Axis Equivalent Circuit.....	9
2-4	q-Axis Circuit, ($x_{qQ} = x_q$).....	10
2-5	q-Axis Circuit, ($x_{qQ} = x_Q$).....	10
2-6	Determination of T_D from Slip Test.....	14
2-7	Connection for the Decaying Current Test.....	14
2-8	Resolving Decaying Current into Two Components.....	16
3-1	Components of V_R in dq and DQ coordinates.....	20
3-2	A Typical Exciter-Voltage Regulator System.....	25
3-3	A Typical Governor-Hydraulic System.....	28
4-1	Algorithm to Determine Q with Dominant Eigenvalue Shift.....	40
5-1	A Typical One-Machine Infinite System.....	42
5-2	Nonlinear Test Results.....	50
6-1	A Typical Four-Machine Power System.....	52
6-2	Nonlinear Tests of the Multi-Machine System.....	62
7-1	Structures of Nominal and Optimally Sensitive Controllers.....	66
7-2	Speed and Torque Angle Gains for the Controllers.....	79
7-3	Nonlinear Test Results.....	80

ACKNOWLEDGMENT

I wish to express my most grateful thanks and deepest gratitude to Dr. Y.N. Yu, supervisor of this project, for his continued interest, encouragement and guidance during the research work and writing of this thesis.

I also wish to thank Dr. E.V. Bohn, Dr. M.S. Davies and Dr. H.R. Chinn for reading the draft, and for their valuable comments. The proof reading of the final draft by Mr. B. Prior is duly appreciated.

Thanks are due to Miss Linda Morris for typing this thesis.

The financial support from the National Research Council and the University of British Columbia is gratefully acknowledged.

I am grateful to my wife Zainab for her encouragement throughout my graduate program.

NOMENCLATURE

General

A	system matrix
B	control matrix
Y	state vector
u	control vector
Q	positive semi-definite symmetric matrix, weighting matrix of Y
R	positive definite symmetric matrix, weighting matrix of u
q	vector, diagonal elements of Q
K	Riccati matrix
G	closed loop system matrix
$\lambda = \xi + j\eta$	eigenvalue vector of G
$\lambda_{i,q}$	sensitivity vector of the eigenvalue λ_i w.r.t. q
S	sensitivity matrix
M	composite matrix as defined in (4.18).
Λ, X, V	eigenvalue vector, eigenvector matrices of M and M'
o	subscript denoting initial condition
\dot{Y}	time derivative of Y
*	superscript denoting conjugate
' or T	superscripts denoting transpose
Δ	prefix denoting a linearized variable
[]	diagonal matrix with elements of each machine
ω_o	synchronous angular velocity: 377 rad/s
p	differential operator

suffices a,d,q armature a-phase, d-axis, and q-axis windings
suffices F,D,Q rotor field, d-axis damper and q-axis damper windings
 A_q sensitivity of matrix A with respect to parameter q.

System parameters (P.U., except as indicated)

Y_N network node admittance matrix
 Z_N network node impedance matrix
 Z_m network node impedance matrix in individual machine coordinates
r+jx tie-line impedance
G+jB terminal load admittance
R's,r's winding resistances in Ω , and per unit
X's,x's self and mutual reactances in Ω , and per unit
L's self and mutual inductances, H
 Z_n armature base ohm, Ω
 x_d, x'_d, x''_d d-axis synchronous, transient and subtransient reactances
 x''_{do} newly defined open field d-axis subtransient reactance
 x_q, x''_q q-axis synchronous, and subtransient reactances
 T'_d, T''_d short circuit d-axis transient and subtransient time constants, s
 T'_{do}, T''_{do} open circuit d-axis transient and subtransient time constants, s
 T_D d-axis damper winding time constant, s
 T''_{qo} open circuit q-axis subtransient time constant, s
 K_A exciter amplifier gain
 T_A exciter amplifier time constant, s

T_E	exciter time constant, s
σ	governor permanent droop
δ_t	governor temporary droop
T_a	gate actuator time constant, s
T_r	dashpot time constant, s
T_g	hydraulic turbine gate time constant, s
T_w	water time constant, s
H	inertia constant
D	damping coefficient

System variables (P.U., except as indicated)

u_E	optimal excitation signal, one-machine infinite system
u_{EC}	conventional excitation control signal
u_G, u'_G	optimal governor control signals with and without dashpot
u_{EI}	one-machine optimal excitation control, multi-machine system
u_{EM}	multi-machine optimal excitation controls, multi-machine system
u_{ES}	optimally sensitive excitation control
$\psi's, i's, v's$	flux linkages, currents, voltages
δ	torque angle, radians
ω_e	angular velocity, electrical rad/s
v_R	exciter regulator voltage
a	gate actuator signal
a_f	dashpot feedback signal

g	gate movement
h	hydraulic head
t_m, t_e	mechanical, electrical torques
v_n, i_n	machine voltages and currents in common coordinates
v_m, i_m	machine voltages and currents in individual coordinates
V_m, I_m	voltage and current matrices with diagonal elements v_m and i_m of each machine
$U_m = U_{md} + jU_{mq}$	sensitivity matrix of v_m with respect to δ .
v_o	infinite bus voltage
v_t	generator terminal voltage
$P + jQ$	generator output power
$V's, v's$	applied voltages in V, and per unit
$U's, u's$	rotational voltages in V, and per unit
$I's, i's$	currents in A, and per unit
V_n, I_n	base armature voltage, current
V_{FB}, V_{DB}, V_{QB}	base field, D-winding and Q-winding voltages
I_{FB}, I_{DB}, I_{QB}	base field, D-winding and Q-winding currents.

1. INTRODUCTION

The stabilization of power systems has become increasingly important because of the increase in the size of power systems, the number of interconnections, the voltage level, the number of large generating units, and the introduction of fast-response excitation systems and dc transmission lines. Much attention has been focussed recently on the application of control signals to the excitation system for stabilization, or stability control, to improve the ability of a power system to return to its synchronous operating equilibrium after a disturbance. These signals can be derived from shaft speed^{1,2,3}, terminal frequency^{4,5,6}, or terminal power^{7,8}. They are used to offset the voltage regulator reference in the transient period with the object of producing positive damping torques on the synchronous machine shaft^{9,10}.

In view of the fast development of control theory, more work must be done to explore the possibility of deriving better methods and techniques for power system stabilization. Optimal linear regulators are designed and quadratic performance functions are chosen^{11,12}.

There are many problems unsolved. Four of them are mentioned below. The first is that in the optimal state regulator design, the choice of the weighting matrix Q associated with the performance function is based entirely upon past experience or guessing. Therefore, the designed controller is not necessarily the best. The second problem is the normal controller is designed for only one particular operating condition, and this condition cannot be estimated prior to a disturbance.

Can an optimal controller be designed to cope with the wide range operating condition? The third problem is the multi-machine dynamics formulation. The problem is not how to obtain a set of state equations but how to avoid the large number of high-order matrix inversions and how to retain all the parameter information for sensitivity investigations. Finally there is the problem of exact representation of synchronous machines and how to determine the circuit parameters from simple field tests. This must be done in order to obtain an accurate evaluation of system dynamic behaviour during and after a disturbance.

This thesis provides some answers to the problems mentioned above. In Chapter 2 the exact equivalent circuits for the synchronous machines are derived from the MKS voltage equations and by the use of per unit systems. Simple field tests to determine the exact machine parameters are then suggested.

The multi-machine state equations are derived in Chapter 3 by relating the transmission network algebraic equations to individual machine dq coordinates. Detailed representation of excitation and governor systems is presented. The one machine infinite bus system is only a special case of the multi-machine system. Dynamic approximation of the formulation is then discussed.

A new technique for the design of optimal regulators is developed in Chapter 4. The choice of the state weighting matrix elements of Q of the performance function is related to the movements of the dominant eigenvalues of the closed loop system. The dominant eigenvalues are shifted to the left on the complex plane within the

practical limits of the controller.

The technique is then applied in Chapter 5 to stabilize a typical one-machine infinite-bus system. Various stabilization schemes are investigated. Optimal excitation and/or governor controls are compared with conventional excitation control. The objective is to find the best way to stabilize a power system.

Some of the stabilization techniques for the one-machine infinite-bus system are further developed for multi-machine system in Chapter 6. Although the one-machine design is more often than not the only case considered, no more difficulty is involved in the formulation or computation for multi-machine systems. Several schemes are investigated, multi-machines with multi optimal controllers or with one optimal controller as compared with multi-machines with individual optimal controllers or an equivalent one-machine with one optimal controller.

An answer to the wide range operating condition problem is given in Chapter 7. An optimally sensitive controller is developed which provides stabilization for a power system which departs widely from normal operation conditions. A comparison is then made of the optimally sensitive control design with other nominal designs.

2. EXACT EQUIVALENT CIRCUITS AND PARAMETERS OF SYNCHRONOUS MACHINES¹³

For stability studies of large power systems, accurate representation of the synchronous machine is required. As pointed out by Canay¹⁴, the conventional equivalent circuits for synchronous machines do not give accurate computed field voltage and current values. He suggested several circuits and showed good agreement between his test and calculated results. His circuit parameters were calculated from design.

Questions arise: How to determine accurate circuit parameters from simple field tests and how to choose the equivalent circuits. The circuits are not unique because of different base volts, base amperes and circuit elements.

In this chapter exact equivalent circuits for synchronous machines are derived from voltage equations in MKS units. Some constraints are then imposed so that the equivalent circuits will lead to the simplest form. A systematic procedure is then developed to determine these circuit parameters from simple field tests.

2.1. d-Axis Exact Equivalent Circuits

Applying Park's transformation, the d-axis voltage equations of a synchronous machine in MKS unit can be written in the form

$$\begin{bmatrix} V_d - U_d \\ V_F \\ 0 \end{bmatrix} = \begin{bmatrix} R_a \\ R_F \\ R_D \end{bmatrix} + p \begin{bmatrix} X_d & X_{aF} & X_{aD} \\ \frac{3}{2}X_{Fa} & X_F & X_{FD} \\ \frac{3}{2}X_{Da} & X_{DF} & X_D \end{bmatrix} \begin{bmatrix} I_d \\ I_F \\ I_D \end{bmatrix} \quad (2.1)$$

The X-matrix is not symmetric¹⁵. Here all X's are reactances of single-phase excitation except X_d which is of three-phase excitation. The numerical coefficient 3/2, and hence the asymmetry of the matrix, results from the a,b and c three-phase excitation on the stator and the F or D single-phase excitation on the rotor.

The matrix form itself suggests that the per unit reactances must, and voltages and currents may, be defined as follows

$$\begin{aligned} x_{dF} &= X_{aF} \frac{I_{FB}}{V_n} & x_{dD} &= X_{aD} \frac{I_{DB}}{V_n} & x_{FD} &= X_{FD} \frac{I_{DB}}{V_{FB}} \\ x_{Fd} &= \left(\frac{3}{2}X_{Fa}\right) \frac{I_n}{V_{FB}} & x_{Dd} &= \left(\frac{3}{2}X_{Da}\right) \frac{I_n}{V_{DB}} & x_{DF} &= X_{DF} \frac{I_{FB}}{V_{DB}} \\ x_d &= X_d \frac{I_n}{V_n} & x_F &= X_F \frac{I_{FB}}{V_{FB}} & x_D &= X_D \frac{I_{DB}}{V_{DB}} \\ r_a &= R_a \frac{I_n}{V_n} & r_F &= R_F \frac{I_{FB}}{V_{FB}} & r_D &= R_D \frac{I_{DB}}{V_{DB}} \\ i_d &= I_d / I_n & i_F &= I_F / I_{FB} & i_D &= I_D / I_{DB} \\ v_d &= V_d / V_n & v_F &= V_F / V_{FB} \end{aligned} \quad (2.2)$$

The matrix of x's is not necessarily reciprocal. To make it reciprocal¹⁶, the following constraints must be imposed,

$$\frac{3}{2} V_n I_n = V_{FB} I_{FB} = V_{DB} I_{DB} \quad (2.3)$$

resulting in

$$\begin{aligned} x_{dF} = x_{Fd} &= \frac{X_{aF}}{Z_n} \left(\frac{I_{FB}}{I_n} \right), \quad x_{dD} = x_{Dd} = \frac{X_{aD}}{Z_n} \left(\frac{I_{DB}}{I_n} \right) \\ x_{FD} = x_{DF} &= \frac{2}{3} \frac{X_{FD}}{Z_n} \left(\frac{I_{FB}}{I_n} \right) \left(\frac{I_{DB}}{I_n} \right) \\ x_d &= \frac{X_d}{Z_n}, \quad x_F = \frac{2}{3} \frac{X_F}{Z_n} \left(\frac{I_{FB}}{I_n} \right)^2, \quad x_D = \frac{2}{3} \frac{X_D}{Z_n} \left(\frac{I_{DB}}{I_n} \right)^2 \\ r_a &= \frac{R_a}{Z_n}, \quad r_F = \frac{2}{3} \frac{R_F}{Z_n} \left(\frac{I_{FB}}{I_n} \right)^2, \quad r_D = \frac{2}{3} \frac{R_D}{Z_n} \left(\frac{I_{DB}}{I_n} \right)^2 \end{aligned} \quad (2.4)$$

$$Z_n = V_n / I_n$$

The d-axis voltage equations can be written now, in per unit, as

$$\begin{bmatrix} v_d - u_d \\ v_F \\ 0 \end{bmatrix} = \begin{bmatrix} r_a + px_d & px_{dF} & px_{dD} \\ px_{Fd} & r_F + px_F & px_{FD} \\ px_{Dd} & px_{DF} & r_D + px_D \end{bmatrix} \begin{bmatrix} i_d \\ i_F \\ i_D \end{bmatrix} \quad (2.5)$$

One of the general d-axis equivalent circuits corresponding to (2.5) is as shown in Fig. 2-1, which reduces to Fig. 2-2, the simplest form, if one sets

$$x_{Fd} = x_{Dd} = x_{FD} \quad (2.6)$$

Note that $x_{d\ell}$, $x_{F\ell}$ and $x_{D\ell}$ are no longer leakage reactances. They are defined as

$$x_{d\ell} = x_d - x_{Fd}, \quad x_{F\ell} = x_F - x_{Fd}, \quad x_{D\ell} = x_D - x_{FD} \quad (2.7)$$

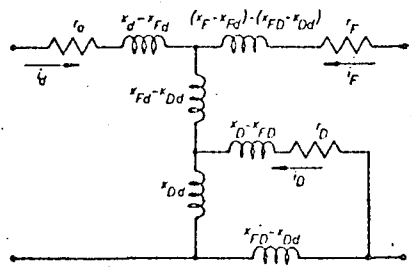


Fig. 2-1 General d-Axis Circuits

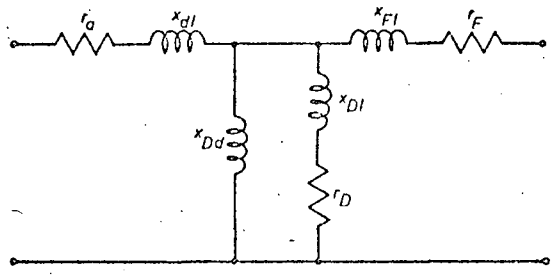


Fig. 2-2 Simplified d-Axis Circuit

The following information, although not needed in the determination of parameters from field tests, is useful in design. From (2.6) the current ratios of (2.4) can be determined as follows

$$\frac{I_{FB}}{I_n} = \frac{3}{2} \frac{X_{aD}}{X_{FD}} \tag{2.8}$$

$$\frac{I_{DB}}{I_n} = \frac{3}{2} \frac{X_{aF}}{X_{FD}} \tag{2.9}$$

Substituting (2.8) and (2.9) into (2.4) and the results into (2.7) the circuit parameters of Fig. 2-2 can be expressed in terms of winding parameters as follows

$$\begin{aligned}
x_{d\ell} &= \frac{X_d}{Z_n} - \frac{3}{2} \frac{X_{aF}}{Z_n} \frac{X_{aD}}{X_{FD}} \\
x_{F\ell} &= \frac{3}{2} \frac{X_{aD}}{X_{FD}} \left(\frac{X_F}{Z_n} \frac{X_{aD}}{X_{FD}} - \frac{X_{aF}}{Z_n} \right) \\
x_{D\ell} &= \frac{3}{2} \frac{X_{aF}}{X_{FD}} \left(\frac{X_D}{Z_n} \frac{X_{aF}}{X_{FD}} - \frac{X_{aD}}{Z_n} \right) \\
x_{FD} &= x_{Dd} = x_{Fd} = \frac{3}{2} \frac{X_{aF}}{Z_n} \frac{X_{aD}}{X_{FD}} \\
r_a &= \frac{R_a}{Z_n}, \quad r_F = \frac{3}{2} \frac{R_F}{Z_n} \left(\frac{X_{aD}}{X_{FD}} \right)^2, \quad r_D = \frac{3}{2} \frac{R_D}{Z_n} \left(\frac{X_{aF}}{X_{FD}} \right)^2
\end{aligned} \tag{2.10}$$

2.2. q-Axis Exact Equivalent Circuits

The q-axis voltage equations for a synchronous machine in MKS unit are as follows

$$\begin{bmatrix} V_q - U_q \\ 0 \end{bmatrix} = \begin{bmatrix} R_a \\ R_Q \end{bmatrix} + p \begin{bmatrix} X_q & X_{aQ} \\ \frac{3}{2} X_{Qa} & X_Q \end{bmatrix} \begin{bmatrix} I_q \\ I_Q \end{bmatrix} \tag{2.11}$$

The X-matrix is again not symmetric¹⁵. While X_q is a reactance of three-phase excitation, X_{aQ} , X_{Qa} and X_Q are of single-phase excitation. The matrix form suggests the following definitions of per unit reactances, voltages and currents

$$\begin{aligned}
x_{qQ} &= X_{aQ} I_{QB} / V_n, \quad x_{Qq} = \left(\frac{3}{2} X_{Qa} \right) I_n / V_{QB} \\
x_q &= X_q I_n / V_n, \quad x_Q = X_Q I_{QB} / V_{QB} \\
r_a &= R_a I_n / V_n, \quad r_Q = R_Q I_{QB} / V_{QB} \\
i_q &= I_q / I_n, \quad i_Q = I_Q / I_{QB}, \quad v_q = V_q / V_n, \quad u_q = U_q / V_n
\end{aligned} \tag{2.12}$$

To make the x-matrix reciprocal¹⁶, the following constraint must be imposed

$$\frac{3}{2} V_n I_n = V_{QB} I_{QB} \quad (2.13)$$

resulting in

$$x_{qQ} = x_{Qq} = \frac{X_{aQ}}{Z_n} \left(\frac{I_{QB}}{I_n} \right), \quad x_q = \frac{X_q}{Z_n}$$

$$x_Q = \frac{2}{3} \frac{X_Q}{Z_n} \left(\frac{I_{QB}}{I_n} \right)^2, \quad r_Q = \frac{2}{3} \frac{R_Q}{Z_n} \left(\frac{I_{QB}}{I_n} \right)^2 \quad (2.14)$$

The per unit q-axis voltage equation now can be written as

$$\begin{bmatrix} v_q - u_q \\ 0 \end{bmatrix} = \begin{bmatrix} r_a + px_q & px_{qQ} \\ px_{Qq} & r_Q + px_Q \end{bmatrix} \begin{bmatrix} i_q \\ i_Q \end{bmatrix} \quad (2.15)$$

The general q-axis equivalent circuit corresponding to (2.15) is as

Fig. 2-3.

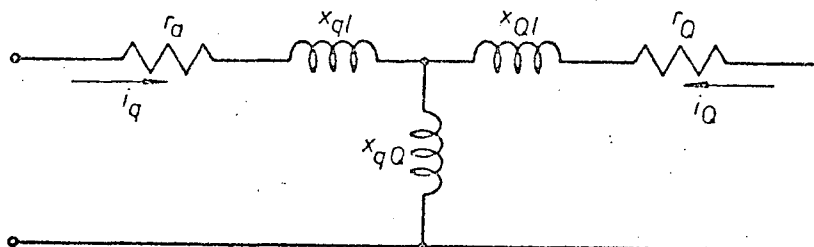


Fig. 2-3 General q-Axis Equivalent Circuits

where

$$x_{ql} = x_q - x_{qQ}, \quad x_{Ql} = x_Q - x_{Qq} \quad (2.16)$$

Although x_{qQ} of Fig. 2-3 exactly represents the mutual reactance and x_{ql} and x_{Ql} the leakage reactances, mathematically,

however, the branch reactance x_{qQ} can be set equal to x_q or x_Q resulting in two simplified equivalent circuits, Figs. 2-4 and 2-5 respectively.

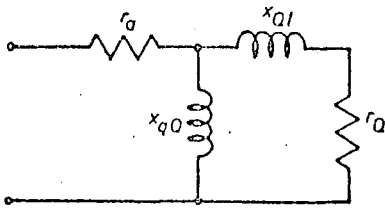


Fig. 2-4 q-Axis Circuits
($x_{qQ} = x_q$)

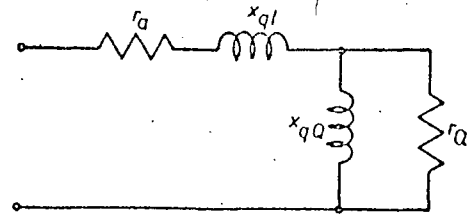


Fig. 3-5 q-Axis Circuit
($x_{qQ} = x_Q$)

The parameters of these two circuits can be easily determined from field tests. They can also be expressed in terms of winding parameters:

Fig. 2-4, $x_{qQ} = x_q$

From (2-14) one has

$$\frac{I_{QB}}{I_n} = \frac{X_q}{X_{aQ}}$$

Hence

$$x_{Ql} = x_Q - x_{Qq} = \left(\frac{2}{3} \frac{X_Q}{X_{aQ}} \frac{X_q}{X_{aQ}} - 1 \right) x_q \quad (2.17)$$

$$r_a = \frac{R_a}{Z_n}, \quad r_Q = \frac{2}{3} \frac{R_Q}{Z_n} \left(\frac{X_q}{X_{aQ}} \right)^2$$

Fig. 2-5, $x_{qQ} = x_Q$

From (2.14) one has

$$\frac{I_{QB}}{I_n} = \frac{3}{2} \frac{X_{aQ}}{X_Q}$$

Hence

$$\begin{aligned}
 x_{q\ell} &= x_q - x_{qQ} = \left(1 - \frac{3}{2} \frac{X_{aQ}}{X_q}\right) x_q \\
 r_a &= \frac{R_a}{Z_n}, \quad r_Q = \frac{3}{2} \frac{R_Q}{Z_n} \left(\frac{X_{aQ}}{X_Q}\right)^2
 \end{aligned}
 \tag{2.18}$$

2.3 Circuit Parameters in Terms of Conventional Parameters

From IEEE test code¹⁷ eight conventional d-axis parameters, i.e., $r_a, x_d, x'_d, x''_d, T'_d, T''_d, T'_{do}$ and T''_{do} can be determined. There are two identities

$$\frac{T'_d}{T'_{do}} = \frac{x'_d}{x_d}, \quad \frac{T''_d}{T''_{do}} = \frac{x''_d}{x'_d}
 \tag{2.19}$$

To determine the seven d-circuit parameters of Fig. 2-2, with IEEE test code, an extra test is necessary. It is suggested to measure a newly defined parameter x''_{do} or a damper time constant T_D .

There are five independent equations for the two sets of parameters¹⁸ besides r_a ;

$$\begin{aligned}
 x_d &= x_{d\ell} + x_{Dd}, \quad x'_d = x_{d\ell} + \frac{x_{Dd}x_{F\ell}}{x_{Dd} + x_{F\ell}} \\
 x''_d &= x_{d\ell} + \frac{x_{Dd}x_{F\ell}x_{D\ell}}{x_{Dd}x_{F\ell} + x_{F\ell}x_{D\ell} + x_{D\ell}x_{Dd}} \\
 \omega_o r_{F'_{do}} &= x_{Dd} + x_{F\ell} \\
 \omega_o r_{D''_{do}} &= x_{D\ell} + \frac{x_{Dd}x_{F\ell}}{x_{Dd} + x_{F\ell}}
 \end{aligned}
 \tag{2.20}$$

If x''_{do} is separately determined, then we have another equation

$$x''_{do} = x_{d\ell} + \frac{x_{Dd}x_{D\ell}}{x_{Dd} + x_{D\ell}}
 \tag{2.21}$$

The solutions of the circuit parameters are

$$x_{d\ell} = x - \sqrt{x^2 - \frac{x'_d x''_d (x_d - x''_{do}) - x_d x''_{do} (x'_d - x''_d)}{(x_d - x''_{do}) - (x'_d - x''_d)}}$$

where

$$x = \frac{x'_d x''_d - x'_d x''_{do}}{(x_d - x''_{do}) - (x'_d - x''_d)} \quad (2.22)$$

and

$$x_{Dd} = x_d - x_{d\ell}, \quad x_{F\ell} = \frac{x'_d - x_{d\ell}}{x_d - x'_d} x_{Dd}$$

$$x_{D\ell} = \frac{(x'_d - x_{d\ell})(x''_d - x_{d\ell})}{x'_d - x''_d} \quad (2.23)$$

$$r_F = \frac{1}{\omega_o T'_{do}} \frac{x_{Dd}^2}{x_d - x'_d}$$

$$r_D = \frac{1}{\omega_o T''_{do}} \frac{(x'_d - x_{d\ell})^2}{x'_d - x''_d}$$

Next, if T_D is separately determined, we have another equation

$$\omega_o T_D = x_D / r_D \quad (2.24)$$

instead of (2.21). The solutions are (2.23) and

$$x_{d\ell} = x'_d - \sqrt{(x_d - x'_d)(x'_d - x''_d) \frac{T''_{do}}{T_D - T''_{do}}} \quad (2.22a)$$

The current ratio I_{FB}/I_n of (2.4) can now be determined, but not

I_{DB}/I_n since there is no way to measure R_D because of the short circuit.

The voltage ratio V_{FB}/V_n can then be determined from (2.3).

The q-circuit parameters can be easily determined. For

Fig. 2-4 we have

$$x_q'' = \frac{x_{qQ} x_{Q\ell}}{x_{qQ} + x_{Q\ell}}, \quad \omega_o T_{qo}'' r_Q = x_{Q\ell} + x_{qQ} \quad (2.25)$$

The solutions are

$$x_{qQ} = x_q, \quad x_{Q\ell} = \frac{x_q x_q''}{x_q - x_q''}, \quad r_Q = \frac{1}{\omega_o T_{qo}''} \frac{x_q^2}{x_q - x_q''} \quad (2.26)$$

For Fig. 2-5 we have

$$x_q'' = x_{q\ell}, \quad \omega_o T_{qo}'' r_Q = x_{qQ}, \quad x_q = x_{qQ} + x_{q\ell} \quad (2.27)$$

The solutions are

$$x_{q\ell} = x_q'', \quad x_{qQ} = x_Q = x_q - x_q'', \quad r_Q = \frac{1}{\omega_o T_{qo}''} (x_q - x_q'') \quad (2.28)$$

2.4. Extra Tests to Determine T_D and x_{do}''

Two test methods are suggested to determine T_D and one to determine x_{do}'' . All methods were tested in the laboratory.

2.4.1. Determination of T_D from a Varying Slip Test

The rotor is driven at various speeds. Positive sequence voltages are applied to the armature winding with the field open. From phase voltage-current ratio equivalent reactances $x_d(s)$ and $x_q(s)$ are approximately determined. Replacing r_D by r_D/s in Fig. 2.2, the imaginary part of the circuit impedance is a function of slip s as follows

$$x_d(s) = x_d - \frac{x_{dD}^2}{r_D} \frac{1}{(\omega_o T_D)^2 + (\frac{1}{s})^2} \quad (2.29)$$

or

$$\frac{1}{x_d - x_d(s)} = \frac{r_D^2}{x_{dD}^2} \left(\frac{1}{s}\right)^2 + \frac{x_D}{x_{dD}} \quad (2.30)$$

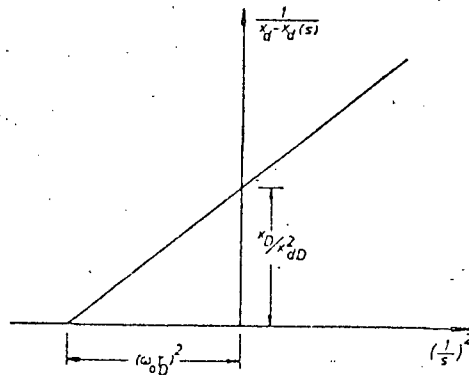


Fig. 2-6 Determination of T_D from Slip Test

which can be plotted as Fig. 2-6 for the determination of T_D . An accurate value of x_d , from open and short circuit tests, must be used for the calculations.

2.4.2. Determination of T_D from Decaying Current Test

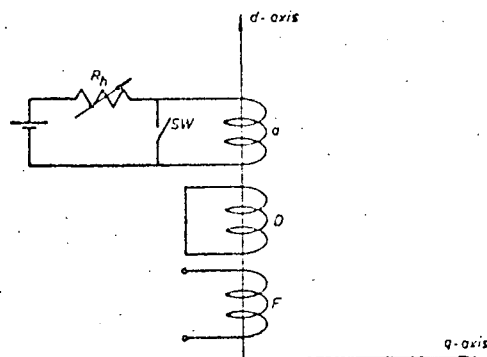


Fig. 2-7 Connection for the Decaying Current Test

Kaminosono and Uyeda's indicial response method¹⁹ is modified to determine T_D . Since a clear step voltage is hard to obtain, a decaying current is used instead. Apply a constant current

to one phase winding in the d-axis position and then suddenly short circuit the armature terminals with the switch Sw in Fig. 2-7. The rheostat R_h protects the power supply.

The voltage equations for Fig. 2-7 in Laplace transform are

$$\begin{bmatrix} 0 \\ 0 \end{bmatrix} = \begin{bmatrix} r_a + sL_d & sL_{dD} \\ sL_{dD} & r_D + sL_D \end{bmatrix} \begin{bmatrix} I_a(s) \\ I_D(s) \end{bmatrix} - \begin{bmatrix} L_d & L_{dD} \\ L_{dD} & L_D \end{bmatrix} \begin{bmatrix} i_{ao} \\ 0 \end{bmatrix} \quad (2.31)$$

where i_{ao} is the initial current in the armature winding. The solution of $I_a(s)$ can be written in a convenient form

$$I_a(s) = \frac{1}{s + \frac{1}{T'_D}} \frac{1}{(s + \frac{1}{T_1})(s + \frac{1}{T_2})} i_{ao} \quad (2.32)$$

where

$$T'_D = T_D(1 - K_{Dd}^2), \quad T_1 T_2 = T_d T'_D, \quad T_1 + T_2 = T_d + T_D \quad (2.32a)$$

and

$$T_D = L_D / r_D, \quad T_d = L_d / r_a, \quad K_{Dd}^2 = L_{Dd}^2 / L_d L_D \quad (2.32b)$$

$I_a(s)$ of (2.32) can be resolved into two components

$$I_a(s) = \frac{i_{10}}{s + \frac{1}{T_1}} + \frac{i_{20}}{s + \frac{1}{T_2}} \quad (2.33)$$

and it can be shown that the initial component current ratio

$$\frac{i_{10}}{i_{20}} = \frac{T_2}{T_1} \frac{T_1 - T'_D}{T'_D - T_2} \quad (2.34)$$

From T'_D , $T_1 + T_2$ of (2.32a) and (2.34), the following solutions are obtained

$$T_d = (i_{10}T_1 + i_{20}T_2)/i_{a0}, T'_d = T_1T_2/T_d, T_D = (i_{10}T_2 + i_{20}T_1)/i_{a0} \quad (2.35)$$

T_1 , T_2 , i_{10} and i_{20} are determined from a semilog plot as Fig. 2-8.

The T_d value from (35) should be checked with

$$T_d = \frac{2}{3} \frac{x_d}{\omega_o r_a} \quad (2.36)$$

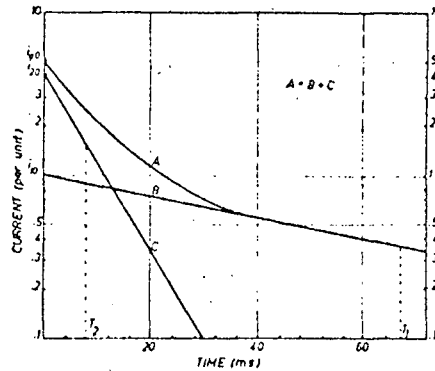


Fig. 2-8 Resolving Decaying Current into Two Components

2.4.3. Determination of x''_{d0}

Dalton and Cameron's method²⁰ to determine x''_d is adapted to determine x''_{d0} . The rotor remains stationary and the field winding is open-circuited. Single phase voltage of rated frequency is applied to each of a pair of stator terminals in turn, leaving the third terminal open. Three such tests are performed with the rotor position fixed throughout the test. The armature voltage and current and the field voltage are recorded in each test.

Let the single-phase reactance X be a function of θ , the angular position of the rotor

$$X = K + M \cos 2\theta \quad (2.38)$$

and let the voltage-current ratio of the three tests be A, B, and C.

It can be shown that

$$K = \frac{A + B + C}{3}, \quad (2.39a)$$

and

$$M = \sqrt{(B-K)^2 + \frac{(C-A)^2}{3}} \quad (2.39b)$$

The open field d-axis subtransient reactance is then given by

$$x''_{do} = \frac{K + M}{2} \quad (2.40)$$

The plus sign should be used if the largest measured reactance, A, B or C, and the largest measured field voltage occur in the same test.

2.5 Laboratory Test Results

The methods thus developed were applied to a small synchronous machine to determine the circuit parameters. From IEEE test code the following d-axis parameters are determined.

$$r_a = 0.72 \Omega, \quad x_d = 16.2 \Omega, \quad x'_d = 2.74 \Omega, \quad x''_d = 2.42 \Omega$$

$$T'_{do} = 0.27s, \quad T''_{do} = 0.027s$$

The per unit values can be obtained when the base ohm Z_n is chosen.

From extra tests the following are determined

$$A \quad T_D = 0.049 \text{ s (varying slip test)}$$

$$B \quad T_D = 0.055 \text{ s (decaying current test)}$$

$$C \quad x''_{do} = 8.18 \Omega \text{ (adapted Dalton and Cameron)}$$

The computed results of d-circuit parameters in ohms are as follows

	x_{Dd}	$x_{d\ell}$	$x_{F\ell}$	$x_{D\ell}$	r_F	r_D
A	15.8	0.40	2.75	14.6	0.182	1.66
B	15.5	0.68	2.38	10.9	0.176	1.28
C	15.9	0.33	2.84	15.5	0.184	1.76

The discrepancy in results of B is attributed to the difficulty of resolving the decaying current into components. The field resistance R_F is 70Ω and the current and voltage ratios are

$$I_{FB}/I_n = 0.0625, \quad V_{FB}/V_n = 24$$

For the q-axis

$$x_q' = 9.71 \Omega, \quad x_q'' = 7.2 \Omega$$

are determined by conventional methods and

$$T''_{qo} = 0.0165 \text{ s}$$

by a decaying current method similar to Fig. 2-7. The computed results of q-axis parameters

$$\text{Fig. 4 } x_{qQ} = 9.71 \Omega, \quad x_{Q\ell} = 27.8\Omega, \quad r_Q = 6.05 \Omega$$

$$\text{Fig. 5 } x_{q\ell} = 7.2 \Omega, \quad x_{qQ} = 2.51 \Omega, \quad r_Q = 0.407 \Omega$$

3. STATE VARIABLE EQUATIONS OF MULTI-MACHINE POWER SYSTEMS²¹

In stabilization studies of large interconnected multi-machine power systems, the system dynamics must be expressed in the state variable form $\dot{Y} = AY + Bu$. Laughton²² suggested a method of building the A matrix from matrix elimination of algebraic and differential equations. Undrill^{23,24} proposed to build up the A matrix from individual system submatrices. Undrill's method requires a matrix inversion of $mn \times mn$ for m machines each described by n -th order equations. The system parameters are not retained in the final formulation. This is also the case in Laughton's formulation.

In this chapter a new multi-machine formulation is proposed. The main objective is to reduce the number of matrix inversions and to keep them of low order. All the system parameters are retained in the final formulation making it convenient for sensitivity and control studies. The synchronous machine parameters are based on an exact equivalent circuit, and can be determined from field tests as described in chapter 2.

3.1. Terminal Voltages and Currents

Let the individual synchronous machine rotating coordinates be d and q and the common rotating coordinates of the complete system be D and Q . Let the terminal voltages and currents of all machines in dq coordinates be a vector v_m and a vector i_m and those in DQ coordinates be a vector v_N and a vector i_N respectively, and let the phase relation

of the k -th machine with respect to the two coordinate systems be as in Fig. 3-1.

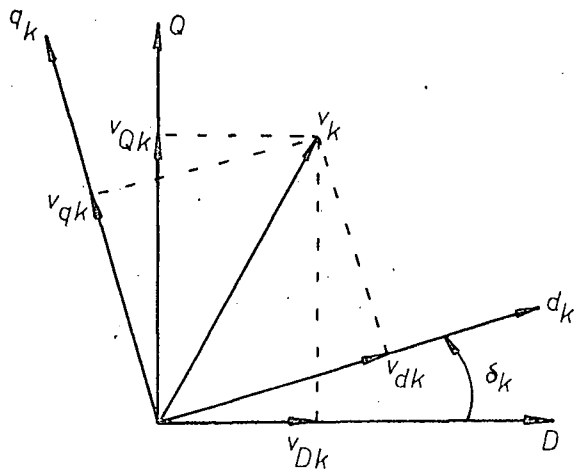


Fig. 3-1 Components of v_k in dq and DQ Coordinates

Then we have for the k -th machine

$$v_{Nk} = \epsilon^{j\delta_k} v_{mk}, \quad i_{Nk} = \epsilon^{j\delta_k} i_{mk} \quad (3.1)$$

and for a group of m machines

$$v_N = [\epsilon^{j\delta}] v_m, \quad i_N = [\epsilon^{j\delta}] i_m \quad (3.2)$$

The transmission system is usually considered as a static network in stability and control studies,

$$i_N = Y_N v_N \quad (3.3)$$

Substituting (3.2) into (3.3) we have

$$v_m = Z_m i_m \quad (3.4)$$

where

$$Z_m = [e^{-j\delta_i}] Z_N [e^{j\delta_j}] \quad (3.5)$$

and

$$Z_N = Y_N^{-1} \quad (3.6)$$

Note that the highest order matrix inversion required in the formulation is Y_N^{-1} . Expanded we have

$$\begin{bmatrix} v_d \\ v_q \end{bmatrix} = \begin{bmatrix} R_m & -X_m \\ X_m & R_m \end{bmatrix} \begin{bmatrix} i_d \\ i_q \end{bmatrix} \quad (3.7)$$

where

$$Z_N = R_N + jX_N, \quad Z_m = R_m + jX_m \quad (3.8)$$

$$\begin{bmatrix} R_m(i,j) \\ X_m(i,j) \end{bmatrix} = \begin{bmatrix} R_N(i,j) & -X_N(i,j) \\ X_N(i,j) & R_N(i,j) \end{bmatrix} \begin{bmatrix} \cos \delta_{ij} \\ \sin \delta_{ij} \end{bmatrix} \quad (3.9)$$

$$\delta_{ij} = \delta_i - \delta_j \quad (3.9a)$$

3.2. Nonlinear Machine Equations

The synchronous machine equations are as follows. For the i -th machine

$$\begin{aligned} v_F &= p\psi_F + r_F i_F \\ v_d &= p\psi_d - r_a i_d - \omega_e \psi_q \\ v_q &= p\psi_q - r_a i_q + \omega_e \psi_d \\ 0 &= p\psi_D + r_D i_D \\ 0 &= p\psi_Q + r_Q i_Q \end{aligned} \quad (3.10)$$

where

$$\begin{bmatrix} \psi_F \\ \psi_d \\ \psi_D \end{bmatrix} = \frac{1}{\omega_o} \begin{bmatrix} x_F & x_{Fd} & x_{FD} \\ x_{dF} & x_d & x_{dD} \\ x_{DF} & x_{Dd} & x_D \end{bmatrix} \begin{bmatrix} i_F \\ -i_d \\ i_D \end{bmatrix} \quad (3.10a)$$

$$\begin{bmatrix} \psi_q \\ \psi_Q \end{bmatrix} = \frac{1}{\omega_o} \begin{bmatrix} x_q & x_{qQ} \\ x_{Qq} & x_Q \end{bmatrix} \begin{bmatrix} -i_q \\ i_Q \end{bmatrix} \quad (3.10b)$$

Note that $-i_d$ and $-i_q$ are used in the synchronous generator equations.

Actually all the notations of (3.10) should be given a suffix "i" for the i-th machine, except for p and ω_o which are common to all machines. The suffix is dropped for clarity. It is also intended that the same equations be used for the description of multi-machine systems. In such a case all the v 's, i 's and ψ 's of (3.10), become column vectors, and x 's and r 's, diagonal matrices. These statements apply also to the rest of the chapter.

The current solutions of (3.10a) and (3.10b) have the form

$$\begin{bmatrix} i_F \\ -i_d \\ i_D \end{bmatrix} = \begin{bmatrix} Y_{FF} & Y_{Fd} & Y_{FD} \\ Y_{dF} & Y_{dd} & Y_{dD} \\ Y_{DF} & Y_{Dd} & Y_{DD} \end{bmatrix} \begin{bmatrix} \psi_F \\ \psi_d \\ \psi_D \end{bmatrix} \quad (3.11a)$$

and

$$\begin{bmatrix} -i_q \\ i_Q \end{bmatrix} = \begin{bmatrix} Y_{qq} & Y_{qQ} \\ Y_{Qq} & Y_{QQ} \end{bmatrix} \begin{bmatrix} \psi_q \\ \psi_Q \end{bmatrix} \quad (3.11b)$$

Note that the solution of currents from (3.10) for individual machines does not involve equations of other machines. The Y matrices of (3.11) are not the inverses of the x matrices of (3.10). If equal per unit mutual reactances are used, the elements of the Y matrices of (3.11a) of individual machines can be determined directly from the d-axis exact equivalent circuit of Fig. 2-2 using the well-known star-mesh relations in network analysis.

Substituting i_d and i_q of (3.11) into (3.7), and the results into v_d and v_q of (3.10), we have

$$p \begin{bmatrix} \psi_d \\ \psi_q \end{bmatrix} = \begin{bmatrix} -R_{dF} Y_{dF} & -R_{dd} Y_{dd} & \omega_e + X_m Y_{qq} & -R_{dD} Y_{dD} & X_m Y_{qQ} \\ -X_m Y_{dF} & -\omega_e - X_m Y_{dd} & -R_{dq} Y_{dq} & -X_m Y_{dD} & -R_{dQ} Y_{dQ} \end{bmatrix} \cdot [\psi_F, \psi_d, \psi_q, \psi_D, \psi_Q] \quad (3.12)$$

where

$$R = \text{Re } Z_m + [r_a] \quad (3.12a)$$

Substituting i_F , i_D and i_Q of (3.11) into v_F , $v_D=0$, and $v_Q=0$ of (3.10), we have

$$\begin{aligned} p\psi_F &= -r_{FF} Y_{FF} \cdot \psi_F - r_{Fd} Y_{Fd} \cdot \psi_d - r_{FD} Y_{FD} \cdot \psi_D + v_F \\ p\psi_D &= -r_{DF} Y_{DF} \cdot \psi_F - r_{Dd} Y_{Dd} \cdot \psi_d - r_{DD} Y_{DD} \cdot \psi_D \\ p\psi_Q &= -r_{Qq} Y_{Qq} \cdot \psi_q - r_{QQ} Y_{QQ} \cdot \psi_Q \end{aligned} \quad (3.13)$$

Thus the transmission line relation (3.7) at the machine terminals has been included in the nonlinear state form of machine equations (3.12) and (3.13).

3.3. Linearized Machine Equations

When equation (3.4) is linearized, it has three terms,

$$\Delta v_m = Z_m \Delta i_m + jZ_m [\Delta \delta_i] i_m - j[\Delta \delta_i] v_m \quad (3.14)$$

which can be written as

$$\Delta v_m = Z_m \Delta i_m + jU_m \Delta \delta \quad (3.14a)$$

where

$$U_m = Z_m I_m - V_m \quad (3.14b)$$

Note that $\Delta\delta$, i_m and v_m are column vectors and $[\Delta\delta]$, I_m and V_m are diagonal matrices. Since

$$v_m = v_d + j v_q, \quad i_m = i_d + j i_q, \quad \psi_m = \psi_d + j \psi_q$$

the voltage equations v_d and v_q of (3.10) can be written as

$$v_m = p\psi_m - [r_a] i_m + j[\omega_e]\psi_m \quad (3.15)$$

After linearization and making use of (3.14a), we have

$$p\Delta\psi_m = [Z_m + (r_a)]\Delta i_m - j[\omega_e]\Delta\psi_m - j[\psi_m] \Delta\omega_e + jU_m \Delta\delta \quad (3.16)$$

Expanded, and with the substitution of i_d and i_q from (3.11) we have

$$p \begin{bmatrix} \Delta\psi_d \\ \Delta\psi_q \end{bmatrix} = \begin{bmatrix} -R_{dF} & -R_{dd} & \omega_e + X_m Y_{qq} & -R_{dD} & X_m Y_{qQ} \\ -X_m Y_{dF} & -\omega_e - X_m Y_{dd} & -R_{dq} & -X_m Y_{dD} & -R_{dQ} \end{bmatrix} \cdot [\Delta\psi_F, \Delta\psi_d, \Delta\psi_q, \Delta\psi_D, \Delta\psi_Q] + \begin{bmatrix} -U_{mq} & [\psi_q] \\ U_{md} & -[\psi_d] \end{bmatrix} \begin{bmatrix} \Delta\delta \\ \Delta\omega_e \end{bmatrix} \quad (3.17a)$$

Equation (3.13), after linearization, becomes

$$p\Delta\psi_F = -r_F Y_{FF} \cdot \Delta\psi_F - r_F Y_{Fd} \cdot \Delta\psi_d - r_F Y_{FD} \cdot \Delta\psi_D + \Delta v_F$$

$$p\Delta\psi_D = -r_D Y_{DF} \cdot \Delta\psi_F - r_D Y_{Dd} \cdot \Delta\psi_d - r_D Y_{DD} \cdot \Delta\psi_D \quad (3.17b)$$

$$p\Delta\psi_Q = -r_Q Y_{Qq} \cdot \Delta\psi_q - r_Q Y_{QQ} \cdot \Delta\psi_Q$$

Equations (3.17a) and (3.17b) are the linearized multi-machine equations in state variable form.

3.4. Exciter and Voltage Regulator System

Fig. 2 shows the block diagram of a typical exciter voltage regulator system

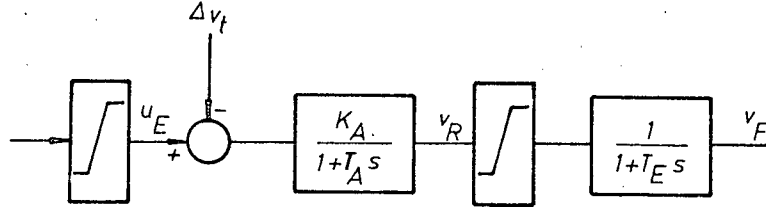


Fig. 3-2 A Typical Exciter-Voltage Regulator System

The corresponding state equations are

$$p\Delta v_F = -\frac{1}{T_E} \Delta v_F + \frac{1}{T_E} \Delta v_R \quad (3.18a)$$

$$p\Delta v_R = -\frac{1}{T_A} \Delta v_R - \frac{K_A}{T_A} \Delta v_t + \frac{K_A}{T_A} u_E \quad (3.18b)$$

Since

$$v_t \Delta v_t = v_d \Delta v_d + v_q \Delta v_q \quad (3.19)$$

then from (3.14a)

$$\begin{bmatrix} \Delta v_d \\ \Delta v_q \end{bmatrix} = \begin{bmatrix} R_m & -X_m \\ X_m & R_m \end{bmatrix} \begin{bmatrix} \Delta i_d \\ \Delta i_q \end{bmatrix} + \begin{bmatrix} -U_{mq} \\ U_{md} \end{bmatrix} \Delta \delta \quad (3.20)$$

Substituting Δi_d and Δi_q of a linearized (3.11) into (3.20), the results into (3.19), and the results into (3.18b), we have

$$\begin{aligned} p\Delta v_R = & A(7,1)\Delta\psi_F + A(7,2)\Delta\psi_d + A(7,3)\Delta\psi_q + A(7,4)\Delta\psi_D \\ & + A(7,5)\Delta\psi_Q - \frac{1}{T_A} \Delta v_R + A(7,8)\Delta\delta + \frac{K_A}{T_A} u_E \end{aligned} \quad (3.21)$$

where

$$A(7,1) = MY_{dF}, \quad A(7,2) = MY_{dd}, \quad A(7,4) = MY_{dD}$$

$$A(7,3) = NY_{qq}, \quad A(7,5) = NY_{qQ},$$

$$A(7,8) = -\left[\frac{K_A}{T_A v_t}\right] (V_q U_{md} - V_d U_{mq}),$$

$$M = \left[\frac{K_A}{T_A v_t}\right] (V_d R_m + V_q X_m), \quad N = \left[\frac{K_A}{T_A v_t}\right] (V_q R_m - V_d X_m) \quad (3.21a)$$

Note that $\left[\frac{K_A}{T_A v_t}\right]$, V_d , and V_q are diagonal matrices built up from the data of individual machines.

So far we have eight state variable sets in the order of

$$(\psi_F, \psi_d, \psi_q, \psi_D, \psi_Q, v_F, v_R, \delta)$$

3.5. Torque Equations

The linearized torque equation in MKS may be written

$$p\Delta\delta = \Delta\omega_e \quad (3.22)$$

$$p\Delta\omega_m = \frac{1}{J} [\Delta T_m - \Delta T_e - \Delta T_D] \quad (3.23)$$

Now if $\Delta\omega_e$'s unit is changed from MKS to per unit, and per unit mechanical torque Δt_m and electrical torque Δt_e are used in the formulation, (3.23) becomes

$$p \frac{\omega_n \Delta\omega_e}{pp} = \frac{T_n}{J} (t_o \Delta t_m - Dt_o \frac{\Delta\omega_e}{\omega_o} - \Delta t_e) \quad (3.23a)$$

where pp is the number of pole pairs, ω_n the base electrical rad/s, T_n the base torque of the complete system, $t_o T_n$ the base operating torque of an individual primemover, and

$$D = \frac{\Delta}{t_o T_n} \frac{\Delta T_D}{\omega_o} \quad (3.23b)$$

Thus we have

$$p\Delta\omega_e = \frac{\omega_o^2}{2H} (t_o \Delta t_m - \Delta t_e - Dt_o \frac{\Delta\omega_e}{\omega_o}) \quad (3.24)$$

where

$$H = \frac{1}{2} J \left(\frac{\omega_o \omega_n}{pp} \right)^2 / P_n \quad (3.24a)$$

and P_n is the base power of the system. Note that

$$\omega_o \omega_n = 120\pi \text{ rad/s} \quad (3.24b)$$

Thus $\omega_n = 1$ if real time is chosen as the base of computation. Otherwise all time constants and H must be multiplied by ω_n . Now since

$$\Delta t_e = \Delta(\psi_d i_q - \psi_q i_d) \quad (3.25)$$

and

$$\Delta t_m = g + 1.5h \quad (3.26)$$

for a hydraulic system, substituting i_d and i_q from (3.11) into (3.25) and the results into (3.24), we have

$$\begin{aligned} p\Delta\omega_e = & A(9,1)\Delta\psi_F + A(9,2)\Delta\psi_d + A(9,3)\Delta\psi_q + A(9,4)\Delta\psi_D \\ & + A(9,5)\Delta\psi_Q - \frac{\omega_o D}{2H} t_o \Delta\omega_e + \frac{\omega_o^2 t_o}{2H} g + \frac{3}{4} \frac{\omega_o^2 t_o}{H} h \end{aligned} \quad (3.27)$$

where

$$\begin{aligned} A(9,1) &= -\frac{\omega_o^2}{2H} [\psi_q] Y_{dF} \\ A(9,2) &= -\frac{\omega_o^2}{2H} ([I_q] + [\psi_q] Y_{dd}) \\ A(9,3) &= \frac{\omega_o^2}{2H} ([\psi_d] Y_{qq} + [I_d]) \\ A(9,4) &= -\frac{\omega_o^2}{2H} [\psi_q] Y_{dD} \\ A(9,5) &= \frac{\omega_o^2}{2H} [\psi_d] Y_{qQ} \end{aligned} \quad (3.27a)$$

$$\begin{aligned}
 -[I_q] &= Y_{qq}[\psi_q] + Y_{qQ}[\psi_Q] \\
 -[I_d] &= Y_{df}[\psi_F] + Y_{dd}[\psi_d] + Y_{dD}[\psi_D]
 \end{aligned}
 \tag{3.27b}$$

The complete state variable sets are

$$(\psi_F, \psi_d, \psi_q, \psi_D, \psi_Q, v_F, v_R, \delta, \omega_e, a, a_f, g, h)
 \tag{3.28}$$

including governor actuator signal a and feedback a_f as in Fig. 3-3.

3.6. Governor-hydraulic System

Fig. 3-3 shows the block diagram of a typical governor-hydraulic system

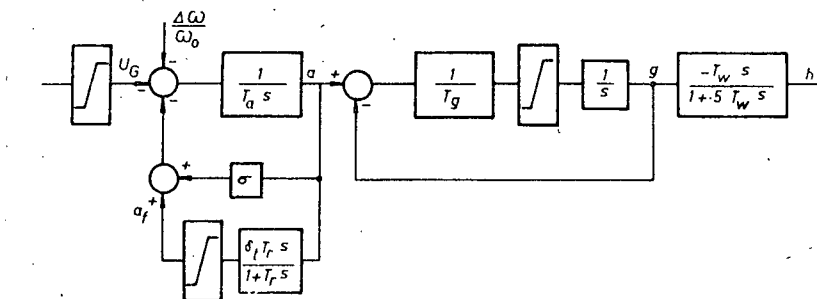


Fig. 3-3 A Typical Governor-Hydraulic System

The corresponding state equations are

$$\begin{aligned}
 pa &= -\frac{\sigma}{T_a} a - \frac{1}{T_a} a_f - \frac{1}{\omega_o T_a} \Delta\omega_e - \frac{1}{T_a} u_G \\
 pa_f &= -\frac{\sigma \delta t}{T_a} a - \left(\frac{1}{T_r} + \frac{\delta t}{T_a}\right) a_f - \frac{\delta t}{\omega_o T_a} \Delta\omega_e - \frac{\delta t}{T_a} u_G \\
 pg &= \frac{1}{T_g} a - \frac{1}{T_g} g \\
 ph &= -\frac{2}{T_g} a + \frac{2}{T_g} g - \frac{2}{T_w} h
 \end{aligned}
 \tag{3.29}$$

3.7. State Equations

There are altogether 13 sets of state variables, (3.28). Each set is an m-vector for an m-machine system. Equations (3.17a), (3.17b), (3.18a), (3.21), (3.22), (3.27) and (3.29) are the complete sets of the system state equations. They are assembled into a matrix equation form as

$$\dot{Y} = A Y + B u, \quad (3.30)$$

$$Y = \Delta (\psi_F \ \psi_d \ \psi_q \ \psi_D \ \psi_Q \ v_F \ v_R \ \delta \ \omega_e \ a \ a_F \ g \ h), \quad (3.30a)$$

$$u = (u_E \ u_a), \quad (3.30b)$$

$$B = \begin{bmatrix} 0 & 0 & 0 & 0 & 0 & 0 & \frac{K_A}{T_A} & 0 & 0 & 0 & 0 & 0 & 0 \\ 0 & 0 & 0 & 0 & 0 & 0 & 0 & 0 & 0 & \frac{-1}{T_a} & \frac{-\delta_t}{T_a} & 0 & 0 \end{bmatrix}, \quad (3.30c)$$

and A is given as equation (3.30d) including (3.21a) and (3.27a) as the auxiliary equations. It is obvious that any other type of exciter and governor systems can be easily incorporated with the rest of the state equations.

3.8. Multi-machine System with an Infinite Bus

For the study of m machines with an infinite bus, the matrix equations (3.4) can be partitioned as

$$\begin{bmatrix} v_m \\ v_\infty \end{bmatrix} = \begin{bmatrix} Z_{mm} & Z_{m\infty} \\ Z_{\infty m} & Z_{\infty\infty} \end{bmatrix} \begin{bmatrix} i_m \\ i_\infty \end{bmatrix} \quad (3.31)$$

Linearization of (3.31) can be written as

A=

$-r_{FF}^Y$	$-r_{Fd}^Y$	0	$-r_{FD}^Y$	0	I	0	0	0	0	0	0	0
$-RY_{dF}$	$-RY_{dd}$	$\omega_e + X_m^Y qq$	$-RY_{dD}$	$X_m^Y qQ$	0	0	$-U_{mq}$	$[\psi_q]$	0	0	0	0
$-X_m^Y dF$	$-\omega_e - X_m^Y dd$	$-RY_{qq}$	$-X_m^Y dD$	$-RY_{qQ}$	0	0	U_{md}	$-[\psi_d]$	0	0	0	0
$-r_{DF}^Y$	$-r_{Dd}^Y$	0	$-r_{DD}^Y$	0	0	0	0	0	0	0	0	0
0	0	$-r_{Qq}^Y$	0	$-r_{QQ}^Y$	0	0	0	0	0	0	0	0
0	0	0	0	0	$-1/T_E$	$1/T_E$	0	0	0	0	0	0
A(7,1)	A(7,2)	A(7,3)	A(7,4)	A(7,5)	0	$-1/T_A$	A(7,8)	0	0	0	0	0
0	0	0	0	0	0	0	0	I	0	0	0	0
A(9,1)	A(9,2)	A(9,3)	A(9,4)	A(9,5)	0	0	0	$\frac{-\omega_0^D}{2H} t_0$	0	0	$\frac{\omega_0^2 t_0}{2H}$	$\frac{3\omega_0^2 t_0}{4H}$
0	0	0	0	0	0	0	0	$-1/\omega_0 T_a$	$-s/T_a$	$-1/T_a$	0	0
0	0	0	0	0	0	0	0	$-\delta_t/\omega_0 T_a$	$-s\delta_t/T_a$	$\frac{-1}{T_r} - \frac{s t}{T_a}$	0	0
0	0	0	0	0	0	0	0	0	$1/T_g$	0	$-1/T_g$	0
0	0	0	0	0	0	0	0	0	$-2/T_g$	0	$2/T_g$	$-2/T_w$

(3.30d)

$$\begin{bmatrix} \Delta v_m \\ \Delta v_\infty \end{bmatrix} = \begin{bmatrix} Z_{mm} & Z_{m\infty} \\ Z_{\infty m} & Z_{\infty\infty} \end{bmatrix} \begin{bmatrix} \Delta i_m \\ \Delta i_\infty \end{bmatrix} + j \left[\begin{bmatrix} Z_{mm} & Z_{m\infty} \\ Z_{\infty m} & Z_{\infty\infty} \end{bmatrix} \begin{bmatrix} I_m & 0 \\ 0 & i_\infty \end{bmatrix} - \begin{bmatrix} V_m & 0 \\ 0 & v_\infty \end{bmatrix} \right] \cdot \begin{bmatrix} \Delta \delta_m \\ \Delta \delta_\infty \end{bmatrix} \quad (3.32)$$

Note that I_m and V_m are diagonal matrices with i_m and v_m as diagonal elements respectively. Since for an infinite bus we have

$$\Delta v_\infty = 0 \quad (3.33a)$$

$$\Delta \delta_\infty = 0 \quad (3.33b)$$

Substituting (3.33) into (3.32) and eliminating Δi_∞ results in

$$\Delta v_m = Z_m \Delta i_m + j U_m \Delta \delta_m \quad (3.14a)$$

where

$$U_m = Z_m I_m - V_m,$$

and

$$Z_m = Z_{mm} - Z_{m\infty} Z_{\infty\infty}^{-1} Z_{\infty m} \quad (3.34)$$

The linearized state equations of the multi-machine system with and without an infinite bus have exactly the same form. But we have to eliminate the infinite bus when the network impedance matrix is expressed in machine's dq coordinates, (3.34).

3.9. Simplification of Power System Dynamics

For system analysis and design purposes it is usually desirable to simplify the dynamic description of the system. Numerical approaches of approximating high order systems by low order systems are available^{25,26}. The principle involved is to retain only the dominant eigenvalues of the exact system in the reduced model. The individual system parametric values, however, are completely lost during the process of numerical approximation.

The simplification of power system dynamics is different in nature. It is governed mainly by the degree of accuracy of describing the flux linkage variations of the synchronous machine windings. Three different approximations are suggested

A: complete description for the system, 7th order synchronous machine, first order voltage regulator and 4th order governor.

B: neglecting damper winding flux linkage variations, i.e.

$$p\psi_D = p\psi_Q = 0$$

C: neglecting damper and armature flux linkage variations

$$p\psi_D = p\psi_Q = 0,$$

and

$$p\psi_d = p\psi_q = 0,$$

C': The same simplification as in model C, except that the system has no governor representation.

The simplification can be easily implemented on the high order system equations (3.30) using matrix elimination technique. The linearized state form equations of a multi-machine power system with 5th order synchronous machine, model B, with second order voltage regulator and exciter system are given in appendix A. From the numerical example of a typical one machine infinite system, Fig. 5-1, it is found that the dominant eigenvalues differ very little from each other in the different simplification methods. Table 3-1 shows the eigenvalues of the typical one machine infinite system of different modelling. Although there are dynamic couplings among all system state variables, roughly, the

model	Eigenvalues			
	#1	#2	#3	#4
A	$.165 \pm j4.69$	-15.2, -3.99	-14.8, -2.24, -1.15, -.034	-847 $\pm j$ 3151, -26.1, -12.4
B	$.229 \pm j4.67$	-16.9, -3.76	-15.1, -2.23, -1.15, -.034	-486 $\pm j$ 1857
C	$.234 \pm j4.67$	-16.9, -3.77	-15.1, -2.23, -1.15, -.034	
C'	$.178 \pm j4.77$	-16.9, -3.68		

Table 3-1 Eigenvalues of the Typical One Machine Infinite System of Different Modelling

4 column eigenvalues correspond to the mechanical system, the voltage regulator and excitation system, the governor system, and the synchronous machine armature and damper windings respectively. Here Column #1 gives the dominant eigenvalues.

4. OPTIMAL LINEAR REGULATOR DESIGN WITH DOMINANT EIGENVALUE SHIFT²⁷

Optimal linear regulators have been designed for power system stabilization^{11,12} and for frequency control²⁸. The performance function J must be chosen in the quadratic form,

$$J = \frac{1}{2} \int_0^{\infty} (Y'QY + u'Ru) dt \quad (4.1)$$

The choice of the weighting matrix Q of (4.1) is entirely left to experience and guessing until satisfactory results are obtained.

In this chapter a new method is developed to determine Q in conjunction with the dominant eigenvalue shift of the closed loop system as far as the practical controllers permit. For the eigenvalue shift of an n -th order system, it is found that it is sufficient to adjust the n diagonal elements of the Q matrix alone without the need of changing the off-diagonal elements. This also leaves out the change in R elements which decide the relative strength of the different control signals and can be left entirely to economical and practical considerations.

4.1. Linear Optimal Regulator Problem

The linear optimal regulator problem may be formulated as follows. Consider the linearized system state equations

$$\dot{Y} = AY + Bu \quad (4.2)$$

Find the optimal control which minimizes the chosen quadratic performance function of (4.1) subject to the system dynamics constraint (4.2). The optimal control is given by²⁹

$$u = -R^{-1}B' K Y \quad (4.3)$$

and the Riccati matrix K satisfies the nonlinear matrix algebraic equation

$$KA + A'K - K B R^{-1}B'K = -Q \quad (4.4)$$

With u decided, the closed loop system equations become

$$\dot{Y} = GY \quad (4.5)$$

where

$$G = A - BR^{-1}B'K \quad (4.6)$$

Thus the eigenvalues of the closed loop system G depend upon the selection of Q for J in (4.1). Consequently the designed optimal controller is not necessarily the best since Q is arbitrarily chosen. On the other hand if Q is adjusted constantly and simultaneously with the dominant eigenvalue shift of the closed loop system, the results will be the best.

4.2. Eigenvalue Shift Policy

The shift is restricted to the real part and to the left.

Let all the eigenvalues of G be ordered as a vector always with the eigenvalue with the largest real part as the first element, λ_1 , and the rest in decreasing order of magnitude. A three-point shift policy is established to avoid unnecessary and undesired large change in Δq which may result in impractical controller gains

1. Assign a negative real shift ϵ to the most dominant eigenvalue λ_1 only.
2. Keep all negative movements of less dominant eigenvalues, e.g., those having negative real parts up to five or ten

times that of λ_1 , within ϵ and damp out all positive movements to the right to avoid their to and fro motion.

3. Relax the movements of the remaining eigenvalues to avoid unusually large controller gains.

4.3. The Shift

Let the incremental change in an eigenvalue λ_i resulting from the change in the diagonal elements of the weighting matrix Q , written as a vector q , be

$$\Delta\lambda_i = \lambda'_{i,q} \Delta q \quad (4.7)$$

since for a conjugate eigenvalue pair

$$\lambda_i = \lambda_{i+1}^* \quad (4.8)$$

their sensitivity coefficients are also conjugate

$$\lambda'_{i,q} = \lambda'^*_{i+1,q} \quad (4.9)$$

Therefore the increments

$$\Delta\lambda_i = \Delta\lambda_{i+1}^* \quad (4.10)$$

There are, in general, k real eigenvalues and $(n-k)/2$ conjugate eigenvalue pairs of the n -th order closed loop system G , and only $(n+k)/2$ independent eigenvalues need to be considered in the shifting process. Let the number be p . Let the p -eigenvalue vector shift be

$$\Delta\lambda = \lambda_{,q} \Delta q \quad (4.11)$$

and let them be separated into real and imaginary parts

$$\Delta\lambda = \Delta\xi + j\Delta\eta \quad (4.12)$$

Then the real part of $\Delta\lambda$ may be written

$$\Delta \xi = S \cdot \Delta q \quad (4.13)$$

where

$$S = \text{Real}(\lambda, q) \quad (4.14)$$

4.4. Determination of Δq

Let the number of dominant eigenvalues be m . Since λ_1 cannot be shifted alone, let a weighted total real shift of the m dominant eigenvalues be

$$\Sigma = \beta_1 \Delta \xi(1) + \beta_2 \Delta \xi(2) + \dots + \beta_m \Delta \xi(m) \quad (4.15)$$

From (4.13) we have

$$\Sigma = \phi' \Delta q \quad (4.16)$$

where

$$\phi = (\phi_1, \dots, \phi_i, \dots, \phi_n)' \quad (4.16a)$$

and

$$\phi_i = \beta_1 S(1,i) + \beta_2 S(2,i) + \dots + \beta_m S(m,i) \quad (4.16b)$$

The β 's are positive numbers satisfying the shift policy point two.

To make Σ negative, Δq is moved in the direction of the steepest descent,

$$\Delta q = -k\phi, \quad k > 0 \quad (4.17)$$

The step size k is so determined that it will have a negative shift for the most dominant eigenvalue λ_1 .

4.5. Sensitivity Coefficients λ, q

Although Chen and Shen³⁰ gave two algorithms to compute λ, q their method requires many computations and large computer storage.

A new sensitivity formula for λ, q is developed in this section. The computation of λ, q and the solution of the Riccati matrix K will be much simplified through an eigenvector matrix X of a composite matrix M ;

$$M = \begin{bmatrix} A & -BR^{-1}B' \\ -Q & -A' \end{bmatrix} \quad (4.18)$$

The composite matrix M has the following properties^{31,32}

1. The $2n$ eigenvalues of M are symmetrically located with respect to both real and imaginary axes of the complex plane. Let the eigenvalue vector Λ of M be partitioned as

$$\Lambda = [\Lambda_I, \Lambda_{II}]' \quad (4.19)$$

where Λ_I has negative real parts and Λ_{II} has positive real parts.

Then we have

$$\Lambda_{II} = -\Lambda_I \quad (4.20)$$

2. The eigenvalues with the negative real parts of M are the same eigenvalues of the optimal closed loop system G , i.e.

$$\Lambda_I = (\lambda_1, \dots, \lambda_i, \dots, \lambda_n)' \quad (4.21)$$

3. The solution of the Riccati matrix equation (4.4) is

$$K = X_{II} X_I^{-1} \quad (4.22)$$

where

$$X = \begin{bmatrix} X_I & X_{III} \\ X_{II} & X_{IV} \end{bmatrix} \quad (4.22a)$$

is the eigenvector matrix of M , and the first column of the eigenvector matrix X corresponds to the stable eigenvalues Λ_I .

4. The eigenvector matrix of M' may be written

$$V = \begin{bmatrix} X_{IV} & X_{II} \\ -X_{III} & -X_I \end{bmatrix} \quad (4.23)$$

Let an eigenvector of the stable eigenvalue λ_i of M be

$$X_i = (X_{II} \quad , \quad X_{III})' \quad (4.24)$$

and that of M' be

$$V_i = (X_{IVi} \quad , \quad -X_{IIIi})' \quad (4.25)$$

Following Faddeev and Faddeeva³³, we have

$$\Delta\lambda_i = \frac{1}{C_i} V_i' \Delta M X_i \quad (4.26)$$

where

$$C_i = V_i' X_i \quad (4.26a)$$

Since in our case

$$\Delta M = \begin{bmatrix} 0 & 0 \\ -\Delta Q & 0 \end{bmatrix} \quad (4.27)$$

We shall have

$$\Delta\lambda_i = \frac{1}{C_i} X_{IIIi}' \Delta Q X_{IIi} \quad (4.28)$$

For the diagonal changes in Q we write

$$\Delta\lambda_i = \lambda_{i,q}' \Delta q \quad (4.29)$$

where

$$\lambda_{i,q} = (\lambda_{i,q1}, \lambda_{i,q2}, \dots, \lambda_{i,qj}, \dots, \lambda_{i,qn})' \quad (4.30)$$

and

$$\lambda_{i,qj} = \frac{1}{C_i} X_{IIIi}(j) X_{IIi}(j) \quad (4.31)$$

where

$$C_i = \sum_{j=1}^n [X_{IVi}(j)X_{Ii}(j) - X_{IIIi}(j)X_{IIi}(j)] \quad (4.32)$$

4.6. Algorithm

The algorithm for the design of linear optimal regulators with dominant eigenvalue shift is summarized in Fig. 4-1.

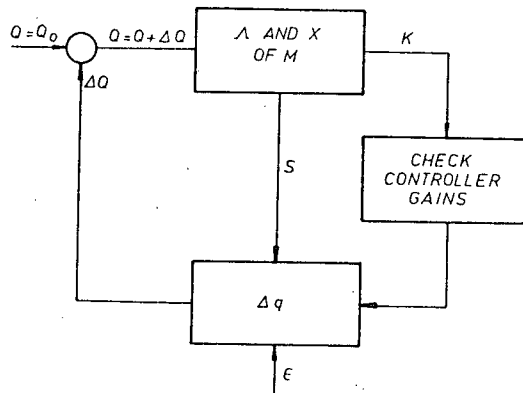


Fig. 4-1 Algorithm to Determine Q with Dominant Eigenvalue Shift

1. Start with a small arbitrary Q.
2. Find the eigenvalues λ and eigenvectors X of the composite matrix M.
3. Calculate K from the stable eigenvectors of X^{32} and check the controller gains at each shift.
4. Find Δq from the sensitivity coefficients λ, q .
5. Update Q and repeat the process until a satisfactory eigenvalue shift is made or until the practical controller's limit is reached.

5. OPTIMAL POWER SYSTEM STABILIZATION THROUGH EXCITATION AND/OR GOVERNOR CONTROL²⁷

In this chapter the linear optimal regulator design technique developed in the previous chapter is applied to the optimal stabilization of a typical one machine-infinite system, Fig. 5-1. Three different optimal stabilization schemes are investigated, the first with an optimal excitation control u_E , the second with optimal governor controls u_G and u'_G , with and without the dash-pot, and the third with u_E plus u'_G control. The linear optimal stabilizing signals thus obtained are tested on a high order nonlinear model of the system with detailed description. It is found from the test results that the optimal controls are more effective than conventional excitation control, that the optimal governor control with the dash-pot removed is just as good as the optimal excitation control, and that the optimal u_E plus u'_G control is the best way to stabilize a power system.

5.1. System Data

A typical one machine-infinite system as shown in Fig. 5-1 is chosen for this study. The regulator-exciter and governor-hydraulic systems are shown in Fig. 3-2 and Fig. 3-3 respectively.

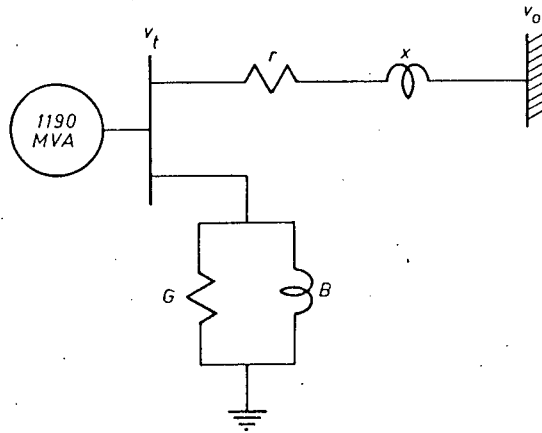


Fig. 5-1 A Typical One-Machine Infinite System

The system data are as follows

r	x	G	B	v_o	v_t	P_o	H	D	
-0.034	.997	.249	.262	1.02	1.05	.952	4.63	0	
x_d	x'_d	x''_d	x_q	x''_q	T''_{do}	T''_{qo}	T_D		
.973	.190	.133	.55	.216	.0436	.0939	.13		
K_A	T_A	T_E	R_F	σ	δ_t	T_a	T_r	T_g	T_w
50	.05	.003	.182	.05	.25	.02	4.8	.50	1.6

The controller constraints are,

exciter amplifier limits (p.u.) 8.83 and -7,

dash-pot signal limits $\pm .025$ p.u.,

governor gate speed limit .1 p.u./sec,

excitation control limits $\pm .12$ p.u. and

governor control limits $\pm .015$ p.u.

For the design the synchronous machine is described as a third order system with $(\psi_F, \delta, \omega)'$ as the state variable vector. This is done by neglecting the flux linkage variations in the armature and damper windings.

5.2. Case 1: u_E Control

The system has an optimal excitation control u_E . The time constant T_E of a solid state exciter is neglected and the voltage regulator of Fig. 3-2 is approximated as a first order system. For the data given, the per unit linear state equations for the complete system are

$$\begin{bmatrix} \Delta \dot{\psi}_F \\ \Delta \dot{v}_F \\ \Delta \dot{\delta} \\ \Delta \dot{\omega} \end{bmatrix} = \begin{bmatrix} -0.196 & 1.0 & -1.39 & -0.003 \\ -50.9 & -20. & 87.0 & -2.4 \\ 0 & 0 & 0 & 1 \\ -2.94 & 0 & -22.6 & -0.008 \end{bmatrix} \begin{bmatrix} \Delta \psi_F \\ \Delta v_F \\ \Delta \delta \\ \Delta \omega \end{bmatrix} + \begin{bmatrix} 0 \\ 1 \\ 0 \\ 0 \end{bmatrix} u_{ex} \quad (5.1)$$

where

$$u_{ex} = 1000 u_E \quad (5.1a)$$

The optimal control signal u_E is found as

$$(-.099\Delta\psi_F - .004\Delta v_F - .62\Delta\delta + 0.1\Delta\omega)$$

The final value of the diagonal elements of Q are

$$(2524 \quad , \quad 0 \quad , \quad 913.6 \quad , \quad 23865)$$

The control weighting R is unity.

The eigenvalues of the initial system without u_E control are

$$(.178 \pm j4.77 \quad , \quad -3.68 \quad , \quad -16.9)$$

and the eigenvalues of the final system with u_E control are

$$(-2.07 \pm j4.9 \quad , \quad -3.85 \quad , \quad -16.7)$$

Thus the dominant eigenvalue pairs are shifted from

$$(.178 \pm j4.77) \quad \text{to} \quad (-2.07 \pm j4.9)$$

5.3. Case 2a: u_G Control, With Dash-pot

The system has an optimal governor control u_G . The 4-th order governor hydraulic system is as Fig. 3-3 and the voltage regulator is approximated as a first order system. For the data given the per unit linear system state equations for the complete system are

$$\dot{Y} = AY + Bu \tag{5.2}$$

where

$$Y = [\Delta\psi_F, \Delta v_F, \Delta\delta, \Delta\omega, a, a_f, g, h]' \tag{5.2a}$$

$$u = u_G \tag{5.2b}$$

$$B = [0, 0, 0, 0, -50, -12.5, 0, 0]' \tag{5.2c}$$

$$A = \begin{bmatrix} -0.196 & 1.0 & -1.39 & -0.003 & 0 & 0 & 0 & 0 \\ -50.9 & -20 & 87.0 & -2.4 & 0 & 0 & 0 & 0 \\ 0 & 0 & 0 & 1 & 0 & 0 & 0 & 0 \\ -2.94 & 0 & -22.6 & -0.008 & 0 & 0 & 38.8 & 58.2 \\ 0 & 0 & 0 & -0.133 & -2.5 & -50 & 0 & 0 \\ 0 & 0 & 0 & -0.033 & -0.625 & -12.7 & 0 & 0 \\ 0 & 0 & 0 & 0 & 2 & 0 & -2 & 0 \\ 0 & 0 & 0 & 0 & -4 & 0 & 4 & -12.5 \end{bmatrix} \tag{5.2d}$$

and R is set

$$R = 1 \tag{5.2e}$$

The optimal control signal u_G is found as

$$\begin{aligned}
 & (.0255 \Delta \psi_F + .0012 \Delta v_F + .126 \Delta \delta - .0254 \Delta \omega \\
 & + .08a - .112 a_f - .3g - .4h)
 \end{aligned}$$

The final values of the diagonal elements of Q are

$$10^{-4} \begin{pmatrix} .56, & 4.8 & .116, & 6.8, \\ .034, & .0019, & .52, & 0 \end{pmatrix}$$

The eigenvalues of the initial system without u_G control are

$$(.23 \pm j4.67, -3.77, -16.9, -.034, -1.149, -2.23, -15)$$

and the eigenvalues of the final system with u_G control are

$$(-1.35 \pm j4.9, -4.1, -16.8, -.049, -1.2, -1.6, -15)$$

Thus the most dominant eigenvalue pairs are shifted from

$$(.23 \pm j4.67) \text{ to } (-1.35 \pm j4.9)$$

The eigenvalue -0.034 , corresponding to a large time constant of the dashpot, has slow response to system disturbance and does not affect the earlier part of system stability.

5.4. Case 2b: u_G' control, without dashpot

The dashpot is removed from Fig. 3-3 for this study. Neglecting the actuator time constant T_a the governor transfer function can be written as $1/(\sigma + T_g' s)$ where $T_g' = \sigma T_g$. For the data given the equations for the complete system are

$$\begin{bmatrix} \dot{\Delta\psi}_F \\ \dot{\Delta v}_F \\ \dot{\Delta\delta} \\ \dot{\Delta\omega} \\ \dot{g} \\ \dot{h} \end{bmatrix} = \begin{bmatrix} -0.196 & 1.0 & -1.39 & -0.003 & 0 & 0 \\ -50.9 & -20 & 87 & -2.4 & 0 & 0 \\ 0 & 0 & 0 & 1 & 0 & 0 \\ -2.94 & 0 & -22.6 & -0.008 & 38.8 & 58.2 \\ 0 & 0 & 0 & -0.1 & -2 & 0 \\ 0 & 0 & 0 & 0.21 & 4 & -12.5 \end{bmatrix} \begin{bmatrix} \Delta\psi_F \\ \Delta v_F \\ \Delta\delta \\ \Delta\omega \\ g \\ h \end{bmatrix} + \begin{bmatrix} 0 \\ 0 \\ 0 \\ 0 \\ -40 \\ 80 \end{bmatrix} \cdot u'_G \quad (5.3)$$

and R is set

$$R = 1$$

(5.3a)

The optimal control signal u'_G is found as

$$\begin{aligned}
 & (.00628\Delta\psi_F + .0002\Delta v_F + .0238\Delta\delta - .01620\Delta\omega \\
 & \quad - .0216g - .1 h)
 \end{aligned}$$

The final values of the diagonal elements of Q are

$$10^{-4}(0, 0, .0063, 1.83, 31.1, 0)$$

The eigenvalues of the initial system without u'_G control are

$$(.715 \pm j4.35, -4.3, -16.8, -.89, -2.8)$$

and the eigenvalues of the final system with u'_G control are

$$(-3.7 \pm j4.9, -3.27, -16.8, -1.18, -2.12)$$

Thus the dominant eigenvalue pairs are shifted from

$$(.715 \pm j4.35) \text{ to } (-3.7 \pm j4.9)$$

5.5. Case 3: u_E Plus u'_G Control

The system under study is the same as that of case 2b except it has both u_E and u'_G control signals. The last term of the system equations becomes

$$\begin{bmatrix} 0 & 1000 & 0 & 0 & 0 & 0 \\ 0 & 0 & 0 & 0 & -40 & 80 \end{bmatrix} \begin{bmatrix} u_E \\ u_G \end{bmatrix} \quad (5.4)$$

where

$$R = 10^3 \begin{bmatrix} 1 & 0 \\ 0 & 160 \end{bmatrix} \quad (5.4a)$$

and is chosen to coordinate the effort of excitation and governor control signals.

The optimal u_E and u_G control signals are found respectively as

$$(-.047\Delta\psi_F - .002\Delta v_F - .319\Delta\delta + 0.05\Delta\omega + .779g + .78h),$$

$$(.005\Delta\psi_F + .0002\Delta v_F + .025\Delta\delta - .0127\Delta\omega - .045g - .094h)$$

The final values of the diagonal elements of Q are

$$(1.42, 0, .0859, 25.8, 82.28, .025)$$

The eigenvalues of the initial system without u_E and u_G control are the same as those of case 2b and the eigenvalues of the final system with u_E and u_G control are

$$(-4.13 \pm j5.33, -3.6, -16.79, -.997, -1.66)$$

Thus the dominant eigenvalue pairs are shifted from

$$(.715 \pm j4.35) \text{ to } (-4.13 \pm j5.33)$$

5.6. Nonlinear Tests

All the optimal stabilizing signals thus obtained are tested on the same system of Fig. 5-1 but described by high order nonlinear differential equations with the synchronous machine as a 7-th order system $(\psi_d, \psi_q, \psi_F, \psi_D, \psi_Q, \delta, \omega)$, excitation and governor systems respectively as Figs. 3-2 and 3-3 with controller constraints. A conventional excitation

control as designed in reference 12

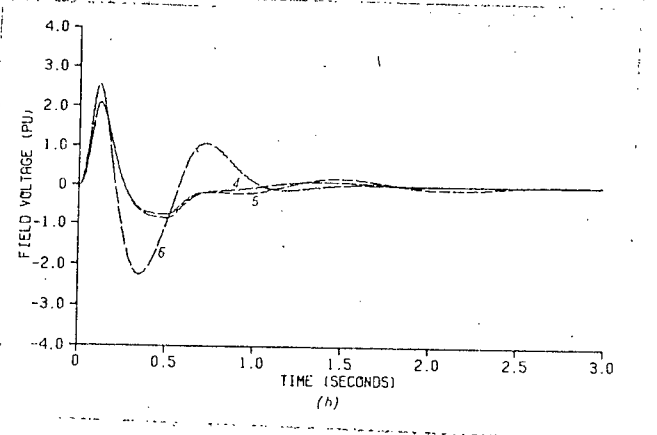
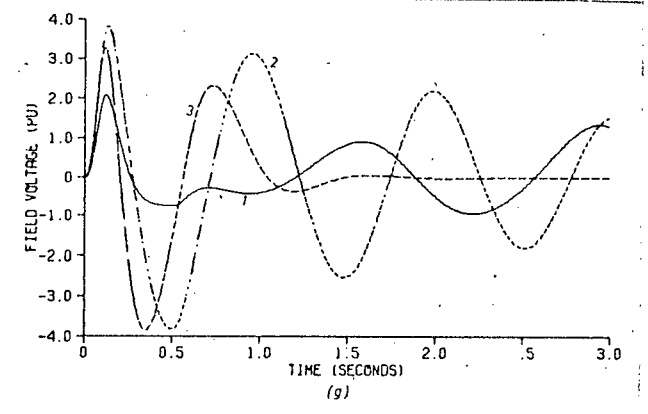
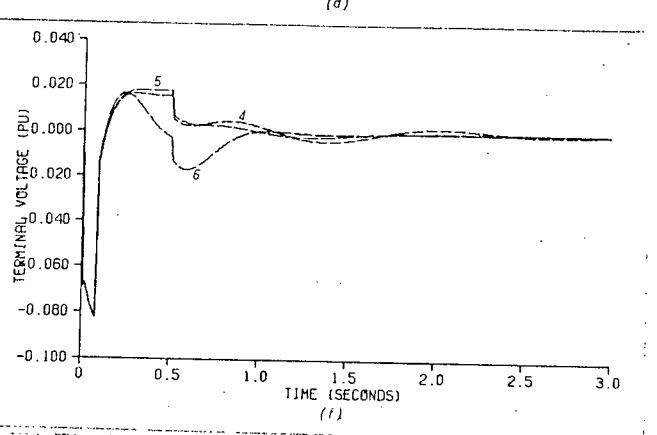
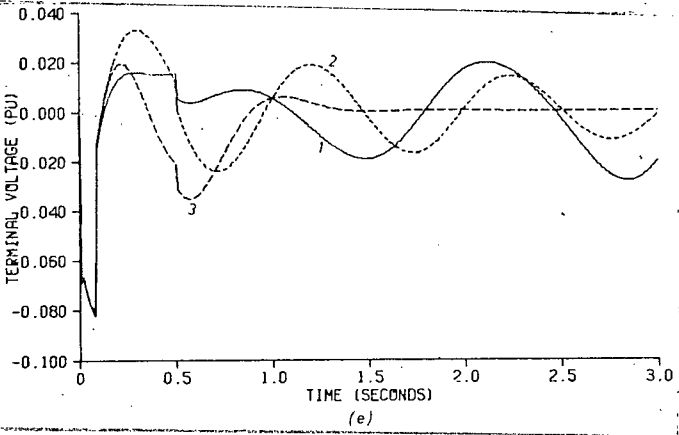
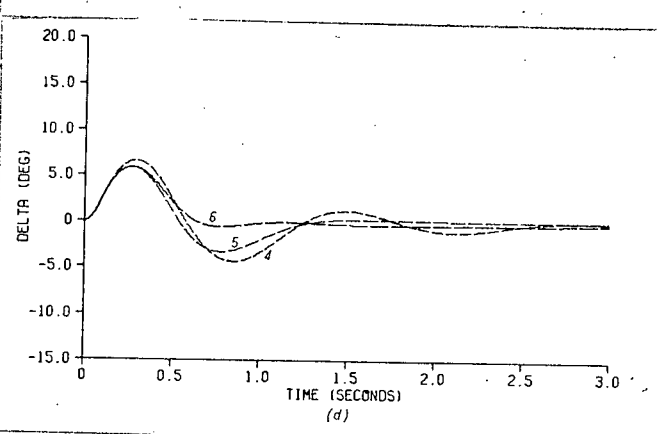
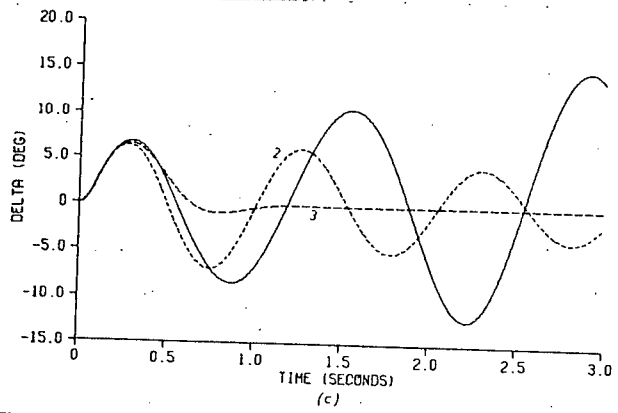
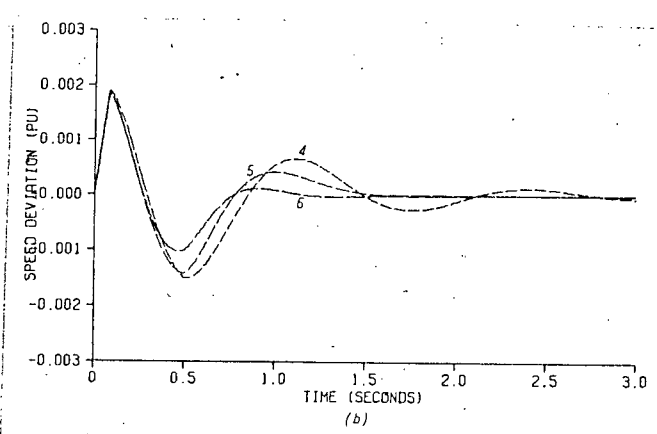
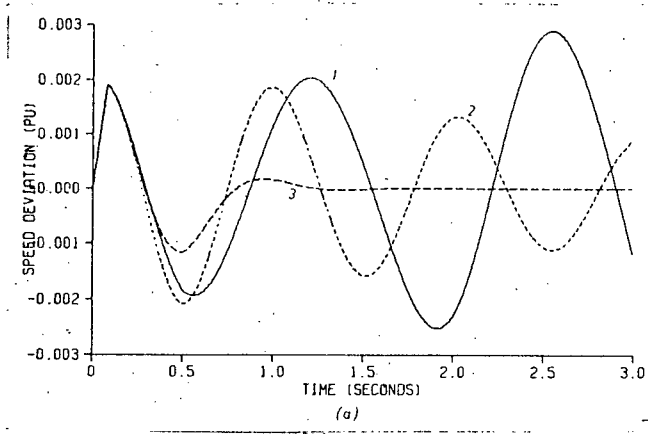
$$u_{EC} = \frac{.04s}{1+.5s} \Delta\omega \quad (5.5)$$

using the speed deviation signal is also included for comparison.

The system disturbance for the tests is as follows: a three-phase fault occurs at one of the system buses and the faulted line is isolated at 5 cycles followed by a system restoration at 30 cycles. The results are summarized in Fig. 5-2. The system responses for the system with conventional and the optimal excitation controls are displayed on the left column of the figures, and the system responses for the system with the optimal governor, and the optimal governor and excitation controls are displayed on the right column of the figures.

From the results, it is observed that:

1. Although the effort of the optimal excitation control signal u_E is smaller than that of the conventional excitation signal u_{EC} , the system with u_E control is much more stable.
2. The optimal governor control signal u'_G for the governor without dashpot provides more damping for the system than that with a dashpot.
3. The optimal excitation and governor signals, u_E and u'_G , when coordinated, provide the best means for stabilizing a power system, i.e., more damping with less effort than either u_E or u'_G control. In other words, for the same amount of effort, the optimal u_E plus u'_G control has the ability to stabilize the system under more severe fault conditions.



Continued...

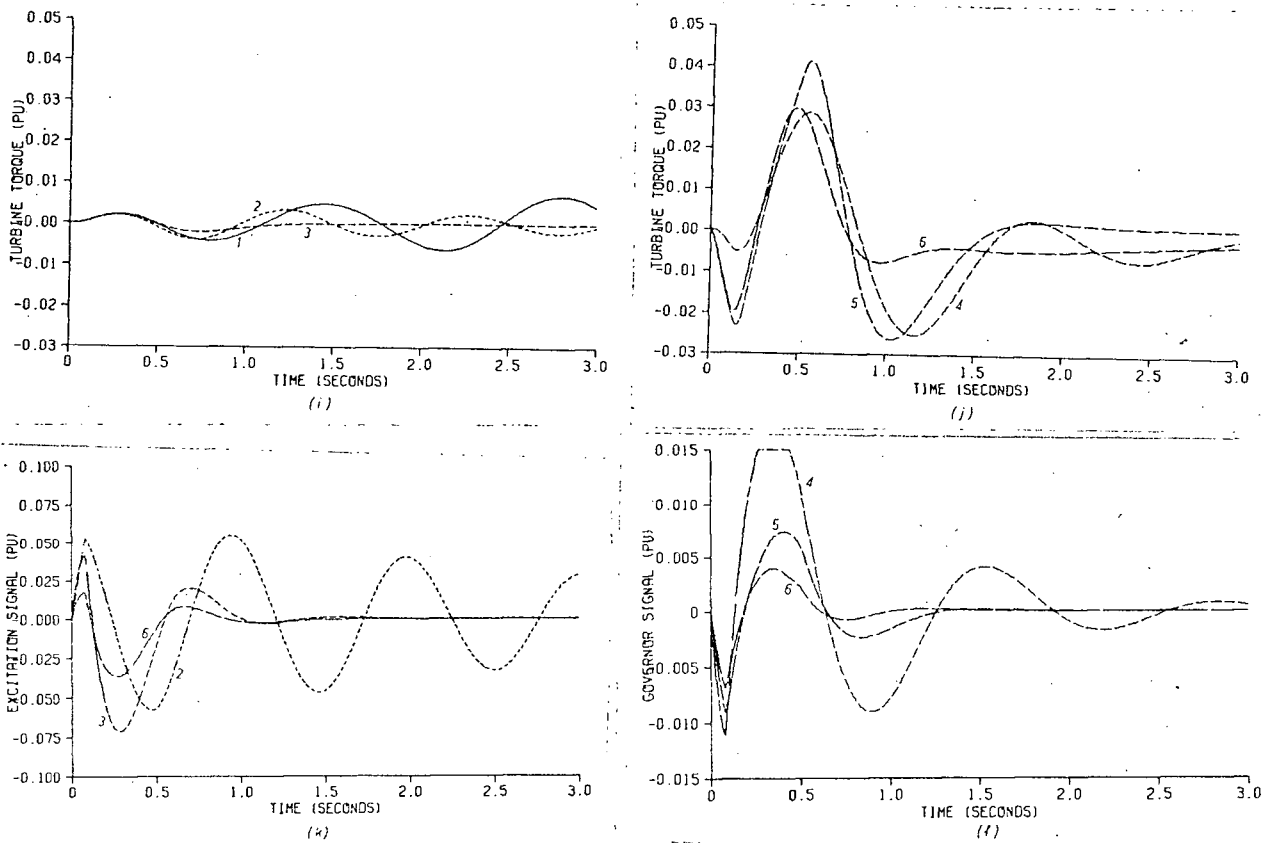


Fig. 5.2 Nonlinear Test Results

1. $u_E = 0$, unstabilized system
2. u_{EC} , conventional excitation control
3. u_E , optimal excitation control
4. u_G , optimal governor control with dashpot
5. u_G' , optimal governor control without dashpot
6. u_E plus u_G' control

6. OPTIMAL STABILIZATION OF A MULTI-MACHINE SYSTEM²¹

The optimal linear regulator design technique of determining the weighting matrix Q in conjunction with the dominant eigenvalue shift, developed in chapter 4, is applied to the optimal stabilization of a multi-machine system. Two systems are investigated, the first with a one machine optimal controller, u_{EI} , and the second with a multi-machine optimal controllers, u_{EM} . Each design is given a nonlinear test on the same multi-machine system. It is found that the multi-machine system with a one machine optimal controller u_{EI} , designed for the multi-machine system is better than a one machine optimal controller, u_E , designed for the same system but approximated as a one machine-infinite system, and that the multi-machine system with a multi-machine optimal controller, u_{EM} , is better still than the multi-machine system with the one machine optimal controller, u_{EI} , designed for multi-machine system.

6.1. System Data and Description

The system under study, Fig. 6-1, is the same as that of reference 12, consisting of one thermo plant (#1), two hydro plants (#2 and #3), and an infinite system equivalent (#4).

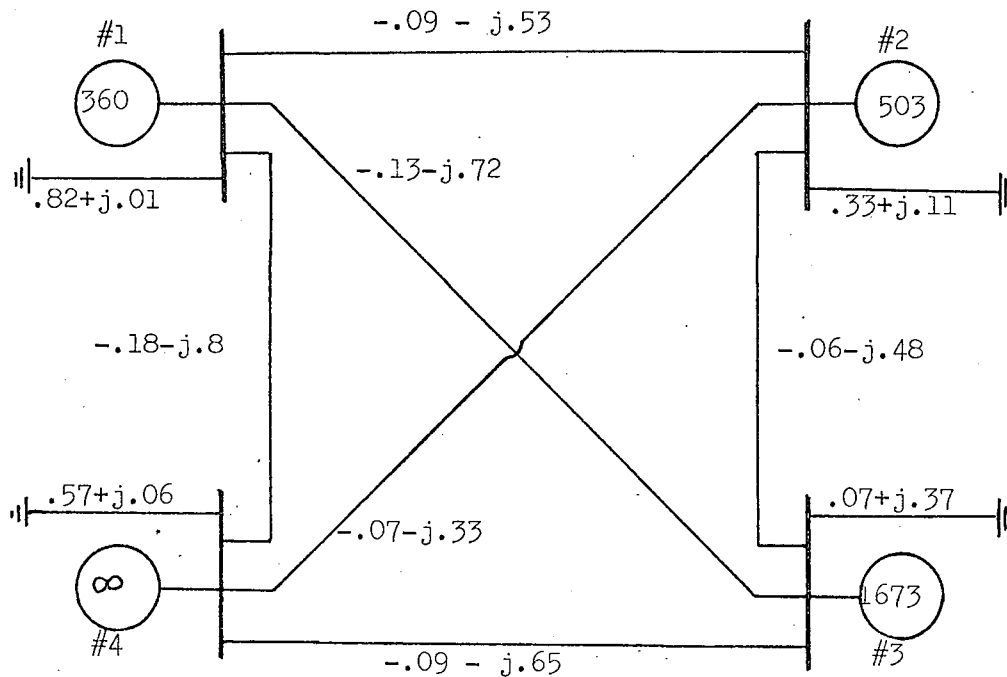


Fig. 6-1. Typical Four-Machine Power System
(Admittances in p.u. on 1000 MVA)

The system data are as follows

Plant	r_a	x_d	x'_d	x''_d	x_q	x''_q	T'_{do}	T''_{do}	T''_{qo}	T_D	H	D
#1	.0019	1.53	.29	.17	1.51	.17	4	.029	.029	.116	2.31	0
#2	.0023	.88	.33	.22	.53	.29	8	.022	.044	.077	3.4	0
#3	.0025	.97	.19	.13	.55	.216	7.76	.044	.094	.131	4.63	0

K_A	T_A	T_E	R_F	V_{Rmax}	V_{Rmin}
13	.21	.15	.129	4.5	0
45	.07	.5	.237	3.5	-3.5
50	.02	.003	.12	8.8	-7

The operating conditions from load flow studies are

Plant	P_o (MW)	Q_o (MVA)	v_{to} (p.u.)	θ (deg.)
#1	26.5	37	1.04	-10.7
#2	518	-31	1.025	11.8
#3	1582	-49.6	1.03	25
#4	410	49.3	1.06	0

For the design each plant is modelled as a fourth-order system $(\psi_F, v_F, \delta, \bar{\omega})$, a third-order synchronous machine plus a first-order exciter-regulator system. The linearized system equations are written as

$$\begin{bmatrix} \dot{Y}_1 \\ \dot{Y}_2 \\ \dot{Y}_3 \end{bmatrix} = \begin{bmatrix} A_{11} & A_{12} & A_{13} \\ A_{21} & A_{22} & A_{23} \\ A_{31} & A_{32} & A_{33} \end{bmatrix} \begin{bmatrix} Y_1 \\ Y_2 \\ Y_3 \end{bmatrix} + B \begin{bmatrix} u_1 \\ u_2 \\ u_3 \end{bmatrix} \quad (6.1)$$

For the data given the numerical values of the A and B matrices are

$$A_{11} = \begin{bmatrix} -.922 & 1 & -.266 & -.009 \\ -2.75 & -2.78 & -1.36 & -.037 \\ 0 & 0 & 0 & 1 \\ -4.95 & 0 & -55.5 & -.039 \end{bmatrix} \quad A_{12} = \begin{bmatrix} .024 & 0 & -.087 & .002 \\ -.158 & 0 & 1.11 & -.011 \\ 0 & 0 & 0 & 0 \\ .222 & 0 & 8.17 & .004 \end{bmatrix}$$

$$A_{13} = \begin{bmatrix} .072 & 0 & -.25 & .003 \\ -.46 & 0 & 2.8 & -.02 \\ 0 & 0 & 0 & 0 \\ .924 & 0 & 17.5 & .02 \end{bmatrix} \quad A_{21} = \begin{bmatrix} .021 & 0 & .121 & .003 \\ -1.1 & 0 & -1.62 & -.015 \\ 0 & 0 & 0 & 0 \\ -2.43 & 0 & 1.37 & -.034 \end{bmatrix}$$

$$A_{22} = \begin{bmatrix} -.21 & 1 & -1.6 & -.005 \\ -1.9 & -1.8 & 9.3 & -.12 \\ 0 & 0 & 0 & 1 \\ -3.1 & 0 & -56 & .032 \end{bmatrix} \quad A_{23} = \begin{bmatrix} .06 & 0 & .46 & .002 \\ -1 & 0 & 1.49 & -.04 \\ 0 & 0 & 0 & 0 \\ .12 & 0 & 29.8 & -.028 \end{bmatrix}$$

	$\Delta\psi_F$	Δv_F	$\Delta\delta$	$\Delta\omega$
plant #1	.011	.018	.348	19.6
plant #2	.023	.536	.284	18.3
plant #3	0	0	.022	.523

The gains of u_{EI} for plant #3 are

	$\Delta\psi_F$	Δv_F	$\Delta\delta$	$\Delta\omega$
plant #1	.0172	-.0128	.88	-.04
plant #2	-.0345	-.0109	-.28	-.14
plant #3	-.154	-.0066	-.878	.18

The eigenvalues of the final multi-machine system are

$$\begin{array}{ccc}
 -1.17 \pm j7.86 & \left| \begin{array}{c} -.3 \pm j7.86 \\ -1.02 \pm j1.25 \end{array} \right| & \begin{array}{c} -1.88 \pm j3.55 \\ -3.6, -16.6 \end{array} \\
 \text{(#1)} & & \text{(#2)} \quad \quad \quad \text{(#3)}
 \end{array}$$

Thus the first two eigenvalues of the last column are shifted from $+1.17 \pm j3.98$ to $-1.88 \pm j3.55$, indicating great improvement in damping of plant #3. The control signal, u_{EI} , also improves the damping of plants #1 and #2.

6.3. Case 2: Multi-Optimal Controllers u_{EM}

One would expect that a multi-machine system with multi-optimal controllers will be better stabilized than the system with only one optimal controller. This is studied as case 2. The multi-optimal controllers are designed, of course, simultaneously considering all machine dynamics.

The diagonal elements of Q determined from the dominant eigenvalue shift are the listed values times 10^{-3} ,

	$\Delta\psi_F$	Δv_F	$\Delta\delta$	$\Delta\omega$
plant #1	.145	.001	2.64	97.2
plant #2	4.65	3.36	3.11	93.6
plant #3	.1	.0007	4.02	88.2

The weighting matrix elements of three plant controls which give the best results are

$$R = \text{diag} (1, 2, 10)$$

The gains of the three control signals are:

$U_{EM}(\#1)$	$\Delta\psi_F$	Δv_F	$\Delta\delta$	$\Delta\omega$
plant #1	-1.06	-.029	-.639	-.18
plant #2	-.052	-.0039	-.588	.0313
plant #3	-.073	-.0026	.127	.137

$U_{EM}(\#2)$	$\Delta\psi_F$	Δv_F	$\Delta\delta$	$\Delta\omega$
plant #1	.0084	-.00427	.539	.0218
plant #2	-.069	-.0399	-.826	-.132
plant #3	-.0406	-.00146	-.0097	-.10

$U_{EM}(\#3)$	$\Delta\psi_F$	Δv_F	$\Delta\delta$	$\Delta\omega$
plant #1	-.00569	-.0072	.38	-.0225
plant #2	-.00832	-.00369	.0718	-.0516
plant #3	-.1123	-.00497	-.718	.1156

The eigenvalues of the final multi-machine system are

$$\begin{array}{ccc}
 -1.01 \pm j7.64 & \left| \right. & -0.448 \pm j7.89 & \left| \right. & -2.05 \pm j4.04 \\
 -1.94 \pm j1.099 & \left| \right. & -1.7 \text{ , } -2.74 & \left| \right. & -3.03 \text{ , } -16.65 \\
 \text{(#1)} & & \text{(#2)} & & \text{(#3)}
 \end{array}$$

There is no doubt that a multi-machine system with multi-optimal controllers, u_{EM} , is better than the system with a one plant optimal controller, u_{EI} .

6.4. Case 3: Approximated One-Machine Optimal Design

For comparison, the u_E optimal excitation control signal of the same power system as cases 1 and 2, but approximated as a one-machine infinite system as in Chapter 5, is recorded here. The control signal

$$u_E = -.099\Delta\psi_F - .004\Delta v_F - .620\Delta\delta + .1\Delta\omega$$

was designed for plant #3 as the one-machine and infinite system. When this signal is applied to plant #3 of the multi-machine system the eigenvalues are

$$\begin{array}{ccc}
 -.084 \pm j7.46 & \left| \right. & -.1 \pm j7.8 & \left| \right. & -3.3 \pm j4.5 \\
 -1.46 \pm j1.15 & \left| \right. & -.63 \pm j1.51 & \left| \right. & -2.88 \text{ , } -15.9 \\
 \text{(#1)} & & \text{(#2)} & & \text{(#3)}
 \end{array}$$

When these results are compared with the eigenvalues of the unstabilized multi-machine system, it is found that the u_E control signal does improve the damping of plant #3, but not much of plant #1 or #2.

6.5. Case 4: Subsystems Optimal Design

One would be curious to know what would happen if all plants had individual u_E control designs. This is to say that all the dynamic coupling of the three plants, off-diagonal elements of the A matrix in (6-1), will be neglected and the individual optimal controllers are designed from

$$\begin{aligned}\dot{Y}_1 &= A_{11}Y_1 + b_1u_1 \\ \dot{Y}_2 &= A_{22}Y_2 + b_2u_2 \\ \dot{Y}_3 &= A_{33}Y_3 + b_3u_3\end{aligned}\tag{6.2}$$

respectively. Applying the dominant eigenvalue shift technique, the individual weighting Q matrices are the listed values times 10^{-3} ; for $R = 1$ in each design,

	$\Delta\psi_F$	Δv_F	$\Delta\delta$	$\Delta\omega$
plant #1	0	0	2.296	72.88
plant #2	$.7 \times 10^{-4}$	$.8 \times 10^{-2}$	2.219	69.38
plant #3	.19	0	.549	12.6

The gains of the individual optimal controllers are

	$\Delta\psi_F$	Δv_F	$\Delta\delta$	$\Delta\omega$
u_E (#1)	-.0738	-.0231	-1.059	-.2018
u_E (#2)	-.0446	-.0182	-.838	-.228
u_E (#3)	-.075	-.0035	-.455	.071

The eigenvalues of the individual closed loop systems are

(#1)	(#2)	(#3)
$-.418 \pm j7.48$	$-.58 \pm j7.52$	$-1.9 \pm j4.766$
$-1.868 \pm j1.25$	$-1.1 \pm j1.16$	$-3.23, -16.6$

Next the eigenvalues of the multi-machine system are:

With u_E (#1) alone

$-.36 \pm j7.42$	$+.014 \pm j7.84$	$-.11 \pm j3.96$
$-1.73 \pm j1$	$-.93 \pm j1.4$	$-3.86, -16.62$

With u_E (#2) alone

$-.04 \pm j7.45$	$-.44 \pm j7.8$	$-.097 \pm j4$
$-1.89 \pm j1.29$	$-.956 \pm j1.15$	$-3.84, -16.62$

With u_E (#3) alone

$-.064 \pm j7.46$	$-.079 \pm j7.83$	$-2.33 \pm j4.08$
$-1.47 \pm j1.25$	$-.778 \pm j1.59$	$-3.24, -16.71$

With all three u_E 's

$-.419 \pm j7.58$	$-.463 \pm j7.843$	$-2.53 \pm j4.47$
$-1.55 \pm j1.136$	$+.169, -2.25$	$-2.95, -16.7$

Although the individual optimal controller provides good damping to the individual plant, the effects on other plants are unpredictable.

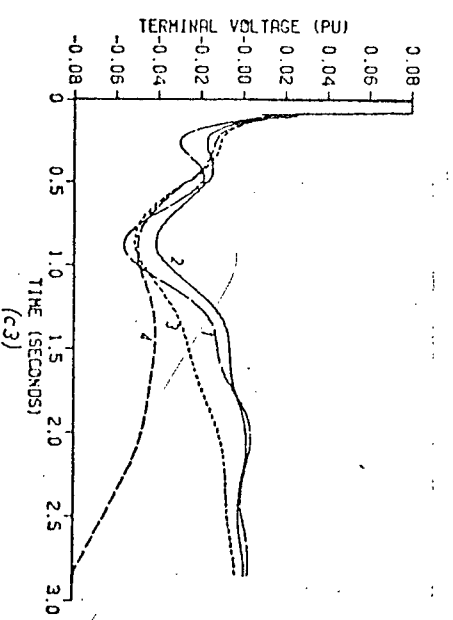
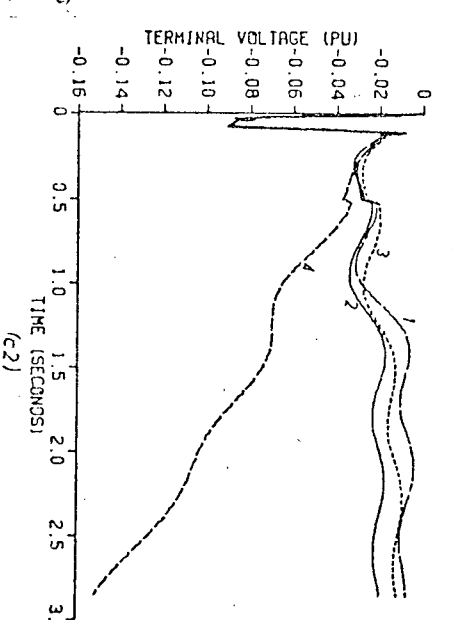
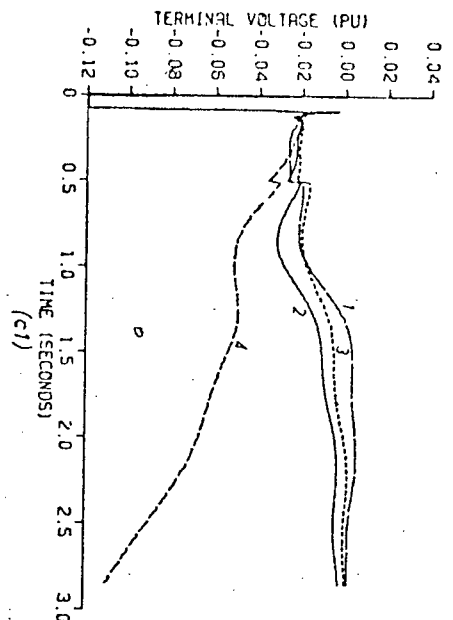
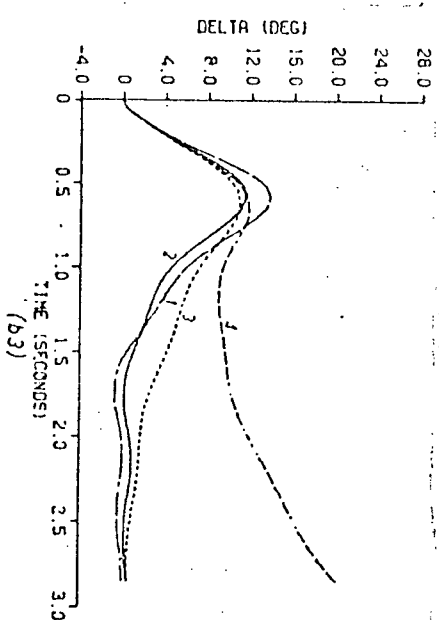
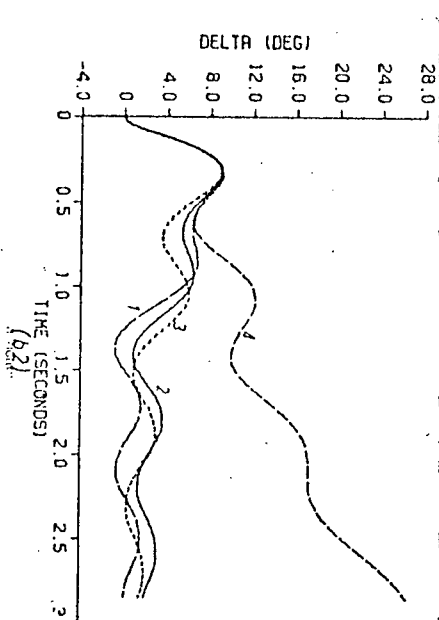
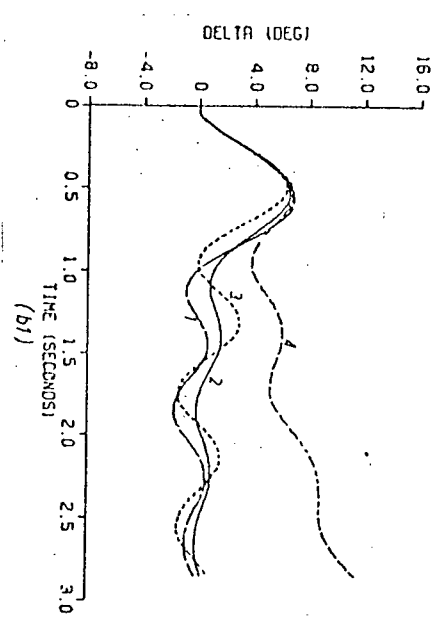
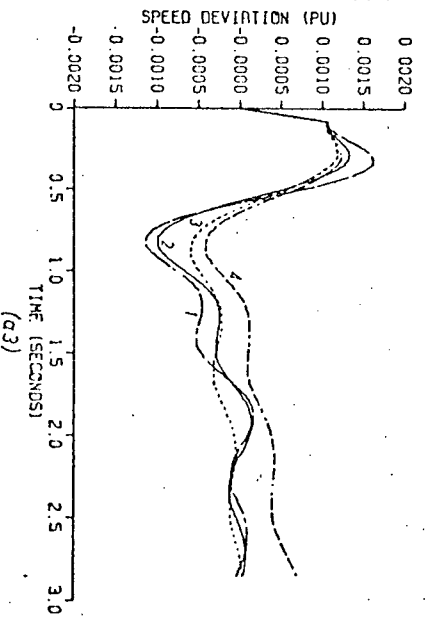
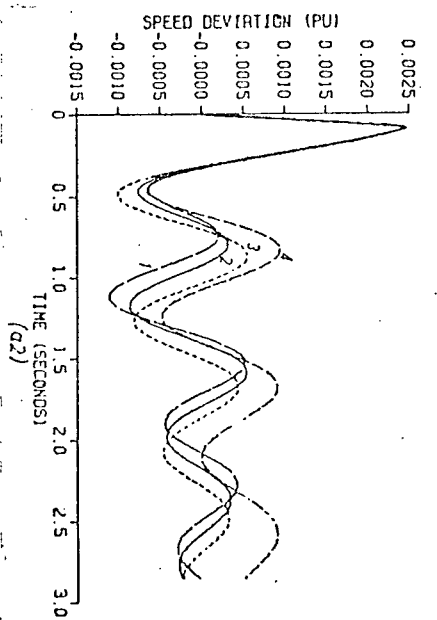
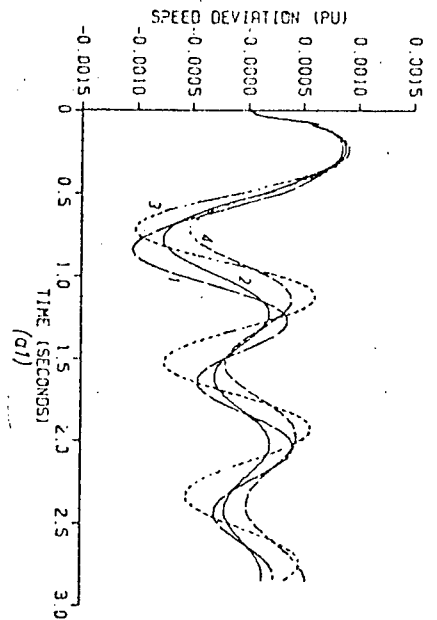
6.6. Nonlinear Tests

The optimal stabilizing signals thus obtained are tested on the

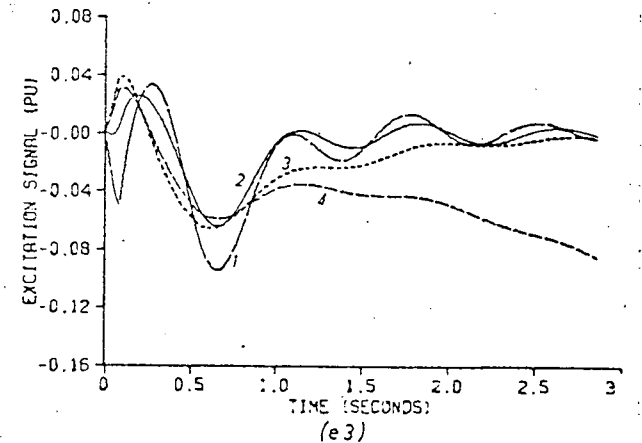
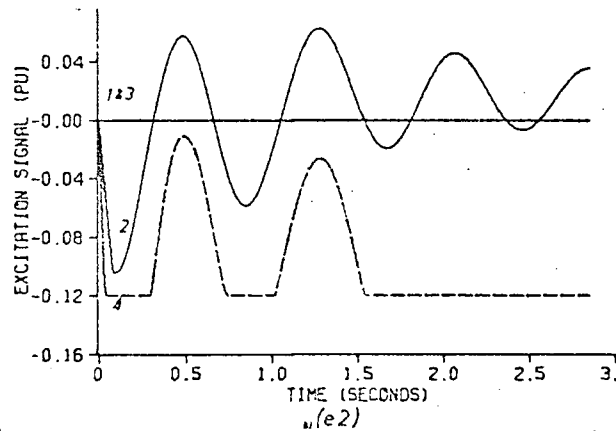
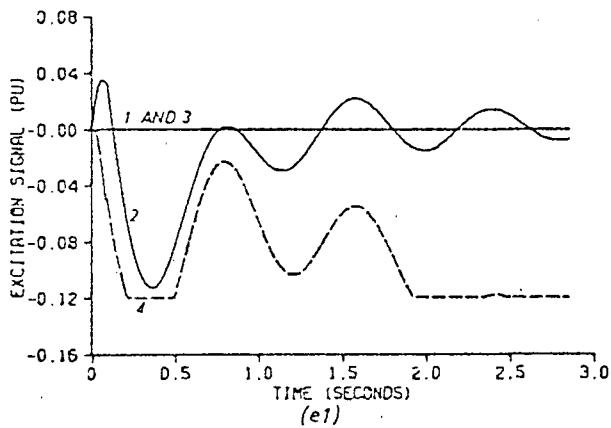
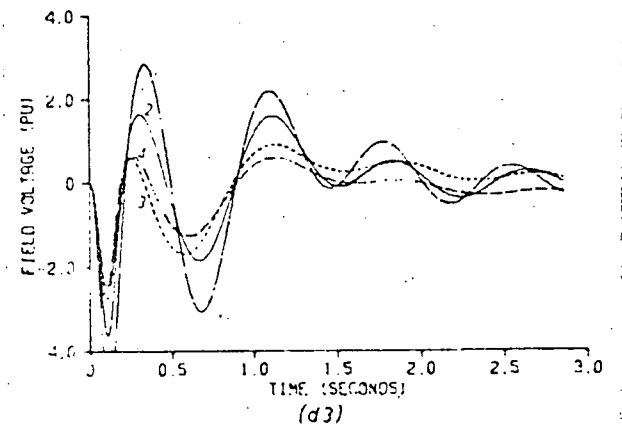
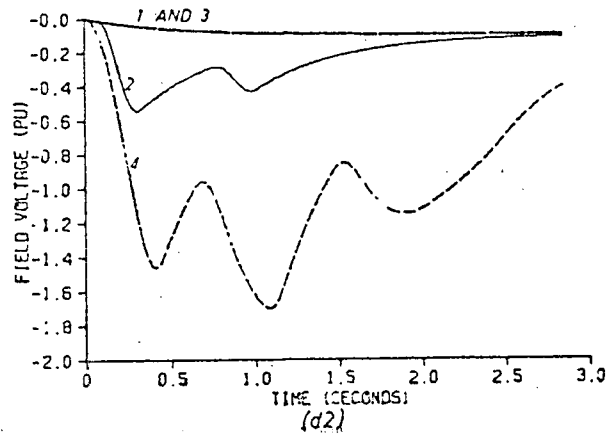
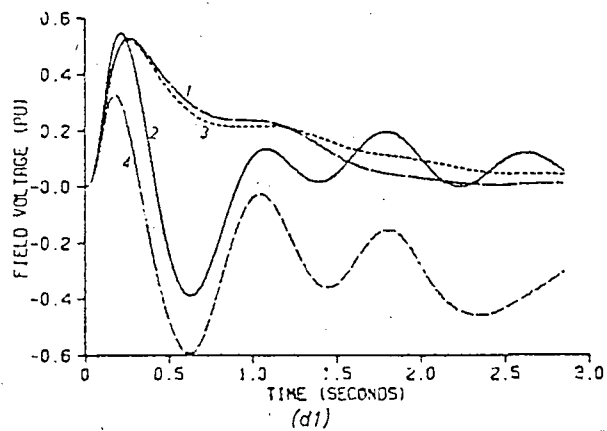
same system of Fig. 6-1 but described by high order nonlinear differential equations including the controller's constraints. The system disturbance for the tests is the same one used in the previous chapter. The test results are summarized in Fig. 6-2.

From the results the following is observed

1. u_E controller, designed for the system approximated as one-machine infinite system, case #3, provides the required damping to plant #3 but not much to other plants.
2. u_{EI} controller, case #1, provides damping to each plant in the system, allowing the controller to stabilize the system for wider fault locations than the case with u_E .
3. u_{EM} controllers, case #2, provide the best stabilization for the whole system with less effort than the case with u_E or u_{EI} .
4. The simplified subsystems controllers fail to stabilize the system.



Continued...



(plant #1)

(plant #2)

(plant #3)

Fig. 6.2 Nonlinear Tests of the Multimachine System (a three-phase fault disturbance)

1. with one optimal control u_{EI} on plant #3
2. with multi-optimal controllers u_{EM}
3. with u_E on plant #3; approximated one machine-infinite system
4. with three individual optimal controllers

7. OPTIMUM STABILIZATION OF POWER SYSTEMS OVER WIDE RANGE OPERATING CONDITIONS³⁴

Nominal system operating conditions were assumed in chapters 5 and 6 for the design of the optimal stabilizing signals. In real power systems the operating conditions are not constant but subject to the load demands over the system. The question arises: How can we design an optimal controller for the power system sensitive to and good for the wide range of operating conditions?

In an attempt to answer this question, an optimally sensitive controller is developed in this chapter. The controller is capable of adjusting its effort in such a manner that optimum system stabilization can always be achieved over the wide range operating conditions. The sensitive controller thus designed under such conditions is tested on the nonlinear model. The results are compared with that of the system with a nominal controller.

7.1. Optimally Sensitive Linear Regulator Design

Constructing a controller which preserves optimality for a nonlinear control system in spite of its parameter variations has been the object of several recent publications^{35,36,37}. The synthesis of linear optimally sensitive controllers by means of perturbation of the Riccati equation (4.4) is dealt with in this chapter.

Let the linearized system equations be

$$\dot{Y} = A(q) Y + Bu \quad (7.1)$$

where q is a vector contains the m changable parameters of the system.

For a quadratic performance function

$$J = \frac{1}{2} \int_0^{\infty} (Y'QY + u'Ru)dt, \quad (4.1)$$

the optimal control law is

$$u^* = -R^{-1} B' K(q) Y \quad (7.2)$$

where $K(q)$ satisfies the Riccati matrix equation,

$$K(q)A(q) + A'(q)K(q) - K(q)BR^{-1}B'K(q) = -Q \quad (7.3)$$

In conventional regulator design the controller is computed for nominal values of the plant parameters q_0

$$u_0 = -R^{-1} B' K(q_0) Y \quad (7.4)$$

for a constant $K(q_0)$. This will be referred to as the nominal optimal control hereafter. But this becomes impractical for system over wide range operating conditions. It implies that it is necessary to recompute K for a large number of sets of the plant parameters q , and the implementation of u^* under every operating condition.

To approximate the control law of (7.2), an optimally sensitive control u_s is introduced. This control u_s tends to track the new optimum of J whenever there is a variation in q . The first order approximation u_s is written as

$$u_{s1} = -R^{-1} B' [K(q_0) + \sum_{i=1}^m K_{q_i} \Delta q_i] Y \quad (7.5)$$

The Riccati sensitivity matrices K_{q_i} are obtained from the differentiation of (7.3) w.r.t. q_i

$$K_{q_i} G + G' K_{q_i} = -C_1 \quad (7.6a)$$

where

$$G = A - BR^{-1}B'K, \quad (7.6b)$$

and

$$C_1 = KA_{q_i} + A'_{q_i} K \quad (7.6c)$$

The second order approximation u_s may be written as

$$u_{s2} = -R^{-1}B'[K(q_0) + \sum_{i=1}^m K_{q_i} \Delta q_i + \frac{1}{2} \sum_{ij} K_{q_i q_j} \Delta q_i \Delta q_j]Y \quad (7.7)$$

where the sensitivity matrices K_{q_i} are computed from equations (7.6), and $K_{q_i q_j}$ from

$$K_{q_i q_j} G + G' K_{q_i q_j} = -C_2 \quad (7.8a)$$

where

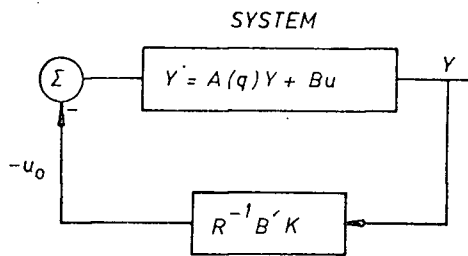
$$\begin{aligned} C_2 = & K_{q_i} G_{q_j} + G'_{q_j} K_{q_i} + K_{q_j} A_{q_i} + A'_{q_i} K_{q_j} + \\ & + K A_{q_i q_j} + A'_{q_i q_j} K \end{aligned} \quad (7.8b)$$

and

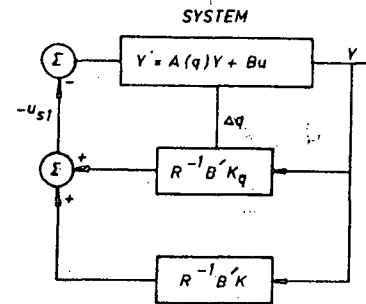
$$G_{q_j} = A_{q_j} - BR^{-1}B'K_{q_j} \quad (7.8c)$$

Equation (7.8a) is obtained by differentiating (7.6a) with respect to q_i . Other matrices of equations (7.6) and (7.8) are computed for $q = q_0$. The procedure can be extended to obtain a controller with higher order approximation by adding more Taylor series terms. However, it will become increasingly difficult to implement the high order controller with a large number of changeable parameters. The structures of the nominal

controller and the optimally sensitive controller of the first order approximation are shown in Fig. 7-1 a and b respectively.



a. Nominal optimal regulator



b. Optimally sensitive regulator

Fig. 7-1 Structures of Nominal and Optimally Sensitive Controllers

The Riccati sensitivity matrices, necessary for the optimal sensitive regulator design, must be computed from the Lyapunov matrix equations of (7.6) and (7.8). A new technique is developed to solve these equations and is given in appendix B. The computational effort is much reduced by the use of the known eigensystem of the closed loop matrix G .

7.2. Sensitivity Equations of the Linearized Power System

For the design of optimally sensitive controllers it is necessary to compute the system sensitivity matrices A_q . This section deals with the derivations of these sensitivity matrices for a general multi-machine power system.

There are in general $(4n-1)$ variables that affect the steady state operating condition for an n machine power system, three terminal

conditions for each machine and (n-1) angular differences between network buses. The operating conditions are expressed in terms of i_d , i_q , v_q , and δ which give the simplest sensitivity expressions. Referring to the multi-machine equations of chapter 3, the deviations of Z_m of (3.5), U_m of (3.14b), M and N of (3.21a), ψ_d and ψ_q of (3.10) for varying operating conditions are as follows

$$\Delta Z_m = jZ_m[\Delta\delta] - j[\Delta\delta]Z_m \quad (7.9)$$

The real and imaginary parts respectively are

$$\Delta R_m = -X_m[\Delta\delta] + [\Delta\delta]X_m \quad (7.9a)$$

and

$$\Delta X_m = R_m[\Delta\delta] - [\Delta\delta]R_m \quad (7.9b)$$

Next,

$$\Delta U_m = Z_m \Delta I_m + \Delta Z_m I_m - \Delta V_m \quad (7.10)$$

using (7.9) and (3.14b), U_m can be written as

$$\Delta U_m = Z_m \Delta I_m + jU_m[\Delta\delta] - j[\Delta\delta]U_m - \Delta V_m \quad (7.11)$$

The real and imaginary parts respectively are

$$\Delta U_{md} = R_m \Delta I_d - X_m \Delta I_q - U_{mq}[\Delta\delta] + [\Delta\delta]U_{mq} - \Delta V_d, \quad (7.11a)$$

and

$$\Delta U_{mq} = X_m \Delta I_d + R_m \Delta I_q + U_{md}[\Delta\delta] - [\Delta\delta]U_{md} - \Delta V_q \quad (7.11b)$$

Note that $V_m = V_d + jV_q$, and $I_m = I_d + jI_q$. They are diagonal matrices with v_m and i_m vector elements of each machine as the diagonal matrix elements. Next,

$$\begin{aligned} \Delta M = & \left[\frac{K_A}{T_A v_t} \right] \{ V_d \Delta R_m + V_q \Delta X_m + \left[\frac{v_q}{v_t} \right]^2 \Delta V_d R_m - \left[\frac{v_d v_q}{v_t^2} \right] \Delta V_d X_m + \\ & + \left[\frac{v_d}{v_t} \right]^2 \Delta V_q X_m - \left[\frac{v_d v_q}{v_t^2} \right] \Delta V_q R_m \} \end{aligned} \quad (7.12)$$

$$\begin{aligned} \Delta N = & \left[\frac{K_A}{T_A v_t} \right] \{ v_q \Delta R_m - v_d \Delta X_m + \left[\frac{v_d}{v_t} \right]^2 \Delta v_q R_m + \\ & + \left[\frac{v_d v_q}{v_t^2} \right] \Delta v_q X_m - \left[\frac{v_q}{v_t} \right]^2 \Delta v_d X_m - \left[\frac{v_d v_q}{v_t^2} \right] \Delta v_d R_m \} \end{aligned} \quad (7.13)$$

Note that $\left[\frac{v_d v_q}{v_t^2} \right]$, $\left[\frac{v_d}{v_t} \right]$, etc. are matrices consisting of diagonal elements computed from data of individual machines. Finally the armature flux linkage variations from the normal steady state operating conditions are as follows,

$$\text{From (3.10) we have} \quad \Delta \psi_d = \frac{1}{\omega_o} (\Delta v_q + r_a \Delta i_q) \quad (7.14)$$

From (3.10b) we have

$$\Delta \psi_q = - \frac{x_q}{\omega_o} \Delta i_q \quad (7.15)$$

In the case of a one machine infinite system, all matrices become scalars and the sensitivity equations (7.9) through (7.13) reduce to

$$\Delta Z_m = \Delta R_m + j \Delta X_m = 0, \quad (7.16)$$

$$\Delta U_{md} = R \Delta i_d - (X_m + x_q) \Delta i_q \quad (7.17)$$

$$\Delta U_{mq} = X_m \Delta i_d + R_m \Delta i_q - \Delta v_q \quad (7.18)$$

$$\begin{aligned} \Delta M = & \frac{K_A}{T_A v_t^3} \{ (v_q^2 R_m - v_d v_q X_m) (x_q \Delta i_q - r_a \Delta i_d) \\ & + (v_d^2 X_m - v_d v_q R_m) \Delta v_q \} \end{aligned} \quad (7.19)$$

$$\begin{aligned} \Delta N = & \frac{K_A}{T_A v_t^3} \{ (v_d^2 R_m + v_d v_q X_m) \Delta v_q \\ & - (v_q^2 X_m + v_d v_q R_m) (x_q \Delta i_q - r_a \Delta i_d) \} \end{aligned} \quad (7.20)$$

The system sensitivity matrices A_q , $q=(i_d, i_q, v_q)'$, for a one machine infinite system of the 5th order synchronous machine model equations of appendix B are as follows.

$$A_{i_d} = \begin{bmatrix} 0 & 0 & 0 & 0 & 0 & 0 & 0 \\ 0 & 0 & 0 & 0 & 0 & -X_m & 0 \\ 0 & 0 & 0 & 0 & 0 & R & 0 \\ 0 & 0 & 0 & 0 & 0 & 0 & 0 \\ M_{i_d} Y'_{dF} & M_{i_d} Y'_{dd} & N_{i_d} Y'_{dq} & 0 & 0 & A_{i_d} (5,6) & 0 \\ 0 & 0 & 0 & 0 & 0 & 0 & 0 \\ 0 & 0 & \frac{\omega_o^2}{2H} & 0 & 0 & 0 & -\frac{v_d + r_a i_d}{2H} D \end{bmatrix} \quad (7.21)$$

$$A_{i_q} = \begin{bmatrix} 0 & 0 & 0 & 0 & 0 & 0 & 0 \\ 0 & 0 & 0 & 0 & 0 & -R_m & -\frac{x_q}{\omega_o} \\ 0 & 0 & 0 & 0 & 0 & -(X_m + x_q) & -\frac{r_a}{\omega_o} \\ 0 & 0 & 0 & 0 & 0 & 0 & 0 \\ M_{i_q} Y'_{df} & M_{i_q} Y'_{dd} & N_{i_q} Y'_{dq} & 0 & 0 & A_{i_q} (5,6) & 0 \\ 0 & 0 & 0 & 0 & 0 & 0 & 0 \\ \frac{\omega_o x_q}{2H} Y'_{dF} & \frac{\omega_o x_q}{2H} (Y'_{dd} - Y'_{dq}) & \frac{\omega_o r_a}{2H} Y'_{dq} & 0 & 0 & 0 & -\frac{v_q + x_q i_d + 2r_a i_q}{2H} D \end{bmatrix} \quad (7.22)$$

$$A_{Vq} = \begin{bmatrix} 0 & 0 & 0 & 0 & 0 & 0 \\ 0 & 0 & 0 & 0 & 1 & 0 \\ 0 & 0 & 0 & 0 & 0 & -\frac{1}{\omega_o} \\ 0 & 0 & 0 & 0 & 0 & 0 \\ M_{Vq} Y'_{dF} & M_{Vq} Y'_{dd} & N_{Vq} Y'_{qq} & 0 & 0 & A_{Vq} (5,6) \\ 0 & 0 & 0 & 0 & 0 & 0 \\ 0 & 0 & \frac{\omega_o}{2H} Y'_{qq} & 0 & 0 & -\frac{i_q}{2H} D \end{bmatrix} \quad (7.23)$$

where

$$M_{id} = -K_A r_a (v_q^2 R_m - v_d v_q X_m) / T_A v_t^3$$

$$N_{id} = K_A r_a (v_q^2 X_m + v_d v_q R_m) / T_A v_t^3 \quad (7.24)$$

$$A_{id} (5,6) = \frac{K_A}{T_A v_t} \left[v_d X_m - v_q R_m - \frac{v_q^2 U_{mq} + v_d v_q U_{md}}{v_t^2} r_a \right]$$

and

$$M_{iq} = K_A x_q (v_q^2 R_m - v_d v_q X_m) / T_A v_t^3$$

$$N_{iq} = -K_A x_q (v_q^2 X_m + v_d v_q R_m) / T_A v_t^3 \quad (7.25)$$

$$A_{iq} (5,6) = \frac{K_A}{T_A v_t} \left[v_d R_m + v_q X_m + \frac{v_q^2 U_{mq} + v_d v_q U_{md}}{v_t^2} x_q \right]$$

and

$$M_{Vq} = K_A (v_d^2 X_m - v_d v_q R_m) / T_A v_t^3$$

$$N_{v_q} = K_A (v_d^2 R_m + v_d v_q X_m) / T_A v_t^3 \quad (7.26)$$

$$A_{v_q} (5,6) = - \frac{K_A v_d}{T_A v_t} - \frac{K_A}{T_A v_t^3} (v_d^2 U_{md} + v_d v_q U_{mq})$$

Although the system sensitivity matrices are derived in terms of the variations Δi_d , Δi_q , and Δv_q , it is always possible to relate these variations to another measurable set through a nonsingular transformation.

For example,

$$\begin{bmatrix} \Delta i_d \\ \Delta i_q \\ \Delta v_q \end{bmatrix} = T^{-1} \begin{bmatrix} \Delta P \\ \Delta Q \\ \Delta v_t \end{bmatrix} \quad (7.27)$$

where

$$T = \begin{bmatrix} v_d - r_a i_d & v_q + x_q i_d & i_q \\ v_q + r_a i_q & -(v_d + x_q i_q) & i_d \\ -\frac{v_d}{v_t} r_a & \frac{v_d}{v_t} x_q & \frac{v_q}{v_t} \end{bmatrix} \quad (7.27a)$$

7.3. Optimally Sensitive Stabilization of a Power System

The one machine infinite system of Fig. 5-1 is chosen for this study. The synchronous machine is described as a 5th order system with ψ_F , ψ_d , ψ_q , δ , and ω as the state variables, appendix A. The voltage regulator is approximated as a first order system by neglecting T_E for the solid state exciter system. Nominal system operating conditions are in p.u.;

$$P_o = .952 \quad , \quad Q_o = .015, \quad \text{and} \quad v_{to} = 1.05 \quad (7.28)$$

The per unit linear state equations for the system at these nominal operating conditions are

$$\dot{Y} = A_o Y + Bu \quad (7.29)$$

where

$$Y = \Delta(\psi_F, \psi_d, \psi_q, v_F, \delta, \omega)' \quad (7.29a)$$

$$B = (0 \quad 0 \quad 0 \quad 1 \quad 0 \quad 0)' \quad (7.29b)$$

For the data given in chapter 5,

$$u = 1000 u_E \quad (7.29c)$$

$$A_o = \begin{bmatrix} -0.660 & 8.55 & 0 & 1 & 0 & 0 \\ 44.9 & -723 & 1230 & 0 & 59.9 & -0.449 \\ 153 & -2848 & -250 & 0 & -497 & -0.954 \\ -418 & 6736 & -368 & -20 & 1125 & 0 \\ 0 & 0 & 0 & 0 & 0 & 1 \\ -5.95 & 62.7 & 86.6 & 0 & 0 & 0 \end{bmatrix} \quad (7.29d)$$

The technique of determining Q developed in chapter 4 is applied to the nominal optimal regulator design of the system. With the weighting factor for control chosen as $R = 1$, Q is found to be

$$Q = \text{diag.}(0 \quad 1.55 \quad 16.3 \quad 0 \quad 737.4 \quad 19084) \quad (7.30)$$

The Riccati matrix is

$$K_o = 10^3 \times \begin{bmatrix} 1.79 & .215 & .08 & .078 & 12.2 & -2.48 \\ .215 & .04 & -.003 & .008 & .863 & -.549 \\ .08 & -.003 & .015 & .005 & 1.1 & .114 \\ .078 & .008 & .005 & .004 & .6 & -.08 \\ 12.2 & .863 & 1.1 & .6 & 133 & -6.5 \\ -2.48 & -.549 & .114 & -.08 & -6.5 & 7.78 \end{bmatrix} \quad (7.31)$$

The nominal optimal control through excitation is

$$u_{E0} = (-.078 \quad -.008 \quad -.005 \quad -.004 \quad -.6 \quad .08) Y \quad (7.32)$$

The system sensitivity matrices, A_q of equations (7.21), (7.22), and (7.23), are computed at the nominal operating conditions. Their values are given in equations (7.33), (7.34), and (7.35). To check the computation of A_q matrices, the system matrix A is computed from the linearized equations (A.3d) and from the sensitivity equation $A = A_o + A_q \Delta q$. A good agreement between both methods is realized over a wide range of system operating conditions.

$$A_{i_d} = \begin{bmatrix} 0 & 0 & 0 & 0 & 0 & 0 \\ 0 & 0 & 0 & 0 & -470 & 0 \\ 0 & 0 & 0 & 0 & 138 & 0 \\ -.17 & 2.75 & 6 & 0 & 202 & 0 \\ 0 & 0 & 0 & 0 & 0 & 0 \\ 0 & 0 & 41 & 0 & 0 & 0 \end{bmatrix} \quad (7.33)$$

$$A_{i_q} = \begin{bmatrix} 0 & 0 & 0 & 0 & 0 & 0 \\ 0 & 0 & 0 & 0 & -137 & -.55 \\ 0 & 0 & 0 & 0 & -678 & -.003 \\ 31 & -505 & -1103 & 0 & 1445 & 0 \\ 0 & 0 & 0 & 0 & 0 & 0 \\ -7.3 & 77 & .22 & 0 & 0 & 0 \end{bmatrix} \quad (7.34)$$

$$A_{v_q} = \begin{bmatrix} 0 & 0 & 0 & 0 & 0 & 0 \\ 0 & 0 & 0 & 0 & 377 & 0 \\ 0 & 0 & 0 & 0 & 0 & -1 \\ -27 & 431 & 943 & 0 & -140 & 0 \\ 0 & 0 & 0 & 0 & 0 & 0 \\ 0 & 0 & 74 & 0 & 0 & 0 \end{bmatrix} \quad (7.35)$$

The Riccati sensitivity matrices K_q are obtained by solving the Lyapunov matrix equations (7.6) using the frequency domain technique developed in appendix B. These matrices are

$$K_{i_d} = 10^3 \times \begin{bmatrix} 1 & .227 & .009 & .044 & -10.4 & -1.85 \\ .227 & .049 & .002 & .01 & -.606 & -.396 \\ .009 & .002 & -.002 & 0 & -.833 & -.094 \\ .044 & .01 & 0 & .002 & -.469 & -.092 \\ -10.4 & -.606 & -.833 & -.469 & -196 & 7.11 \\ -1.85 & -.396 & -.094 & -.092 & 7.11 & 1.32 \end{bmatrix} \quad (7.36)$$

$$K_{i_q} = 10^3 \times \begin{bmatrix} 1.49 & .074 & .045 & .056 & 13.4 & .333 \\ .074 & -.013 & -.003 & .002 & 1.14 & .292 \\ .045 & -.003 & .015 & .004 & .756 & .161 \\ .056 & .002 & .004 & .002 & .578 & .046 \\ 13.4 & 1.14 & .756 & .578 & 112 & -3.73 \\ .333 & .292 & .161 & .046 & -3.73 & -4.54 \end{bmatrix} \quad (7.37)$$

$$K_{v_q} = 10^3 \times \begin{bmatrix} -.654 & -.03 & -.022 & -.031 & 13.1 & 1.51 \\ -.03 & .04 & -.025 & -.004 & .836 & -.267 \\ -.022 & -.025 & .013 & 0 & 1.23 & .242 \\ -.031 & -.004 & 0 & -.001 & .613 & .085 \\ 13.1 & .836 & 1.23 & .613 & 241 & -6.61 \\ 1.51 & -.267 & .242 & .085 & -6.61 & -.918 \end{bmatrix} \quad (7.38)$$

The first order optimally sensitive excitation control, equation (7.5), is then designed

$$u_{ES} = (-.078 \quad -.008 \quad -.004 \quad -.6 \quad .08) Y + \\ + 10^{-3} (\Delta i_{d_o}, \Delta i_{q_o}, \Delta v_{q_o}) \begin{bmatrix} -44 & -9.7 & -.07 & -1.9 & 470 & 92 \\ -56 & -1.5 & -3.7 & -2.4 & -580 & -46 \\ 31 & 4.2 & -.34 & 1.3 & -613 & -85 \end{bmatrix} \cdot Y \quad (7.39)$$

The control can be expressed in terms of ΔP_o , ΔQ_o , and Δv_{t_o} instead of Δi_{d_o} , Δi_{q_o} , and Δv_{q_o} through the transformation

matrix T, equation (7.27),

$$T = \begin{bmatrix} .446 & 1.17 & .814 \\ .953 & -.895 & .399 \\ -.001 & .234 & .905 \end{bmatrix} \quad (7.40)$$

The results are

$$u_{ES} = (-.078 \quad -.008 \quad -.005 \quad -.004 \quad -.6 \quad .08) Y + \\ + 10^{-3} (\Delta P_o, \Delta Q_o, \Delta v_{t_o}) \begin{bmatrix} -77 & -8.9 & -2.6 & -3.3 & 50 & 51 \\ -10 & -6 & 1.1 & -.43 & 468 & 73 \\ 108 & 15 & 1.4 & 4.6 & -928 & -172 \end{bmatrix} Y \quad (7.41)$$

For comparison the controller gains of the optimal signal u_E^* , equation (7.2), for different operating conditions are computed and compared with the resultant gains of the optimally sensitive controller u_{ES} , in table 7-1. The speed and torque angle gains for both signals are plotted in figure 7-2. It is clear that the optimally sensitive controller u_{ES} gains adjust themselves to cover the wide range operating conditions and to match the absolute optimal controllers u_E^* gains. The dominant eigenvalues for the system with the different controllers at different operating conditions are given in table 7-2. While a reduction of stability of the system is observed when it departs from the nominal operating condition, the optimally sensitive controller u_{ES} provides better results than the nominal optimal controller u_{EO} . Although u_E^* provides the best stability, it is impractical to implement as stated before, on the other hand there is no difficulty to implement u_{ES} , it is just as good as

u_{E}^* except for the worst operating condition ($P_o = 1.25$, $Q_o = .45$,
 $v_{t_o} = 1.05$).

system operating conditions ($v_{t_o} = 1.05$)		$P_o = 1.25$ $Q_o = .45$	$P_o = 1.2$ $Q_o = .34$	$P_o = 1.15$ $Q_o = .25$	$P_o = .952$ Nominal $Q_o = .015$	$P_o = .7$ $Q_o = -.15$	$P_o = .5$ $Q_o = -.225$	$P_o = .3$ $Q_o = -.256$	
Controller gains $\times 10^3$	K_{ω}	u_{ES}	128	117	107	80.1	56.3	44.9	41.3
		u_{E}^*	160	134	117	80.1	61	53.9	49.9
	K_{δ}	u_{ES}	-376	-434	-479	-603	-682	-691	-648
		u_{E}^*	-148	-316	-420	-603	-660	-664	-661
	K_{v_F}	u_{ES}	-4.7	-4.49	-4.29	-3.57	-2.6	-1.9	-1.2
		u_{E}^*	-5.18	-4.77	-4.45	-3.57	-2.75	-2.1	-1.5
	K_{ψ_q}	u_{ES}	-5.18	-5.19	-5.17	-4.96	-4.4	-3.9	-3.15
		u_{E}^*	-4.57	-4.88	-5	-4.96	-4.3	-3.56	-2.5
	K_{ψ_d}	u_{ES}	-13	-11.9	-10.9	-7.74	-4.5	-2.5	-.96
		u_{E}^*	-16.7	-13.9	-11.9	-7.74	-5.1	-3.8	-2.9
	K_{ψ_F}	u_{ES}	-104	-99.5	-94.9	-77.8	-55.8	-38.3	-21.6
		u_{E}^*	-117	-107	-99	-77.8	-58.8	-45.3	-31

Table 7-1 Controller Gains For u_{ES} and u_{E}^*
at Different Operating Conditions

Table 7-2 Dominant Eigenvalues of the System with the Different Controllers

Operating Conditions $v_t = 1.05$ P_o Q_o	$u_E=0$	u_{E0}	u_{ES}	u_E^*
1.25 .45	.717+j2.86 -4.8 -16.8	1.49 -4+j4.3 -17.16	.137 -4+j3.8 -17	-2.1 -3.2+j3.1 -16.9
1.2 .34	.56+j3.47 -4.5 -16.9	.467 -3.56+j4.37 -17.15	-1.1 -3.3+j3.9 -17	-2.6 -2.7+j3.7 -16.9
1.15 .25	.44+j3.9 -4.2 -16.9	-.449 -3.1+j4.43 -17.1	-2 -2.8+j4.1 -17	-2.7 -2.5+j4.1 -16.97
Nominal .952 .015	.17+j4.8 -3.6 -16.9	-1.98+j4.99 -2.89 -16.96	-1.98+j4.99 -2.89 -16.96	-1.98+j4.99 -2.89 -16.96
.7 -.15	.023+j5.2 -3.4 -16.8	-1.39+j5.3 -4.4 -16.6	-1.6+j5.3 -2.7 -16.9	-1.56+j5.3 -2.96 -16.89
.5 -.225	-.02+j5.27 -3.4 -16.8	-1.04+j5.3 -5.57 -16.1	-1.28+j5.4 -2.6 -16.97	-1.22+j5.37 -3.1 -16.8
.3 -.256	-.023+j5.25 -3.4 -16.7	-.66+j5.2 -6.8 -15.56	-.83+j5.3 -2.7 -17	-.83+j5.3 -3.3 -16.7

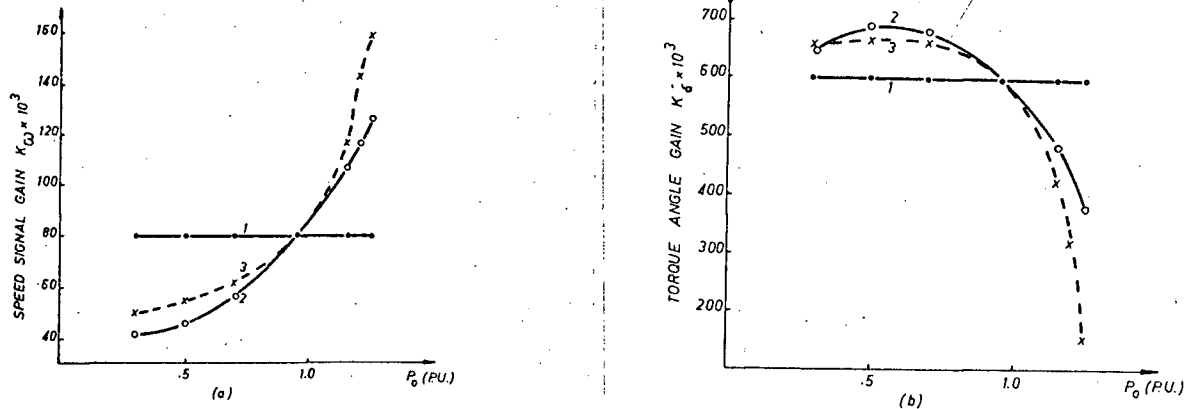


Fig. 7-2 Speed and Torque Angle Gains for the Controllers

(1) u_{EO}

(2) u_{ES}

(3) u_E^*

Both controllers u_{EO} and u_{ES} are tested on the nonlinear model of the system on two operating conditions,

$$P_o = .952, \quad Q_o = .015, \quad v_{t_o} = 1.05 \text{ (Nominal)} \quad (7.28)$$

and

$$P_o = 1.2, \quad Q_o = .34, \quad v_{t_o} = 1.05 \quad (7.42)$$

The system disturbance is the same as in chapter 5. The test results are summarized in Fig. 7-3. While the optimally sensitive controller u_{ES} maintains system stability for the operating conditions of (7.42), the nominal controller u_{EO} fails to do so.

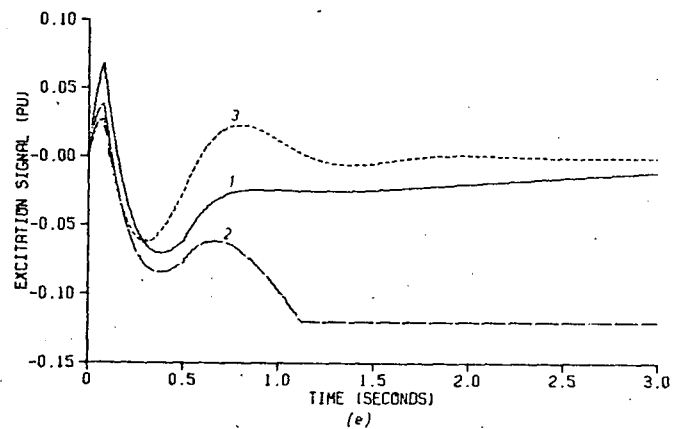
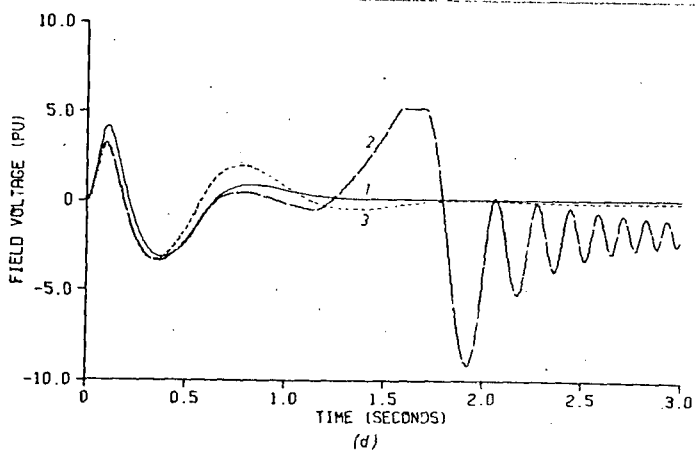
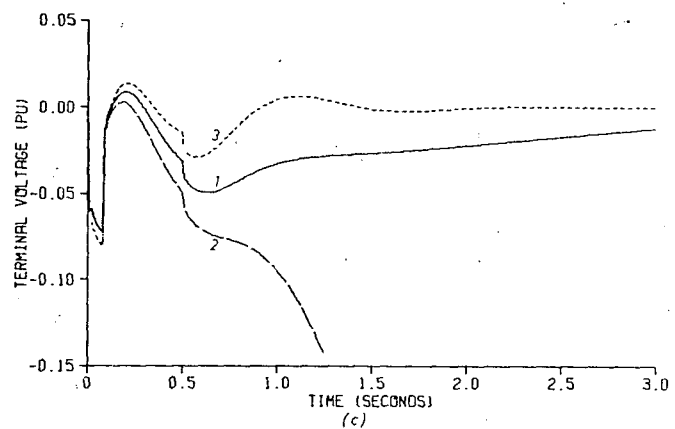
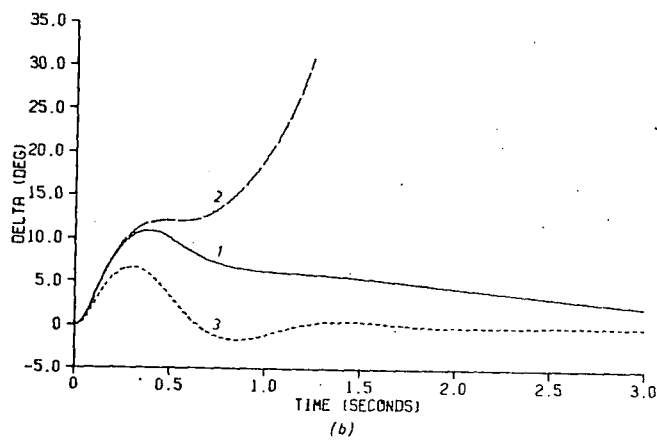
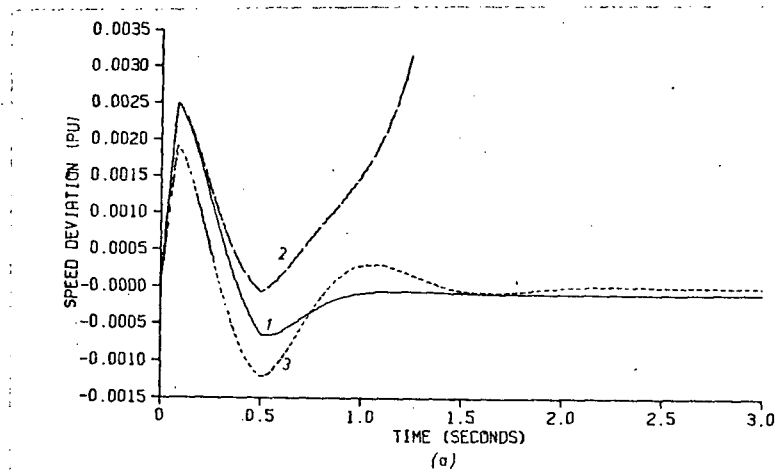


Fig. 7-3 Nonlinear Test Results

- (1) Nominal operating conditions, u_{EO} or u_{ES}
- (2) Nominal optimal control u_{EO} , for $P = 1.2$
- (3) Optimally sensitive control u_{ES} , for $P = 1.2$

8. CONCLUSIONS

An exact representation of synchronous machines is presented and a step by step derivation of the exact equivalent circuit given in Chapter 2. It is found that an extra test with the IEEE test code is needed to determine the d-circuit synchronous machine parameters. Three different methods are suggested, a varying slip test or a decaying current test to determine the D-damper time constant T_D , or an adaptation of Dalton and Cameron's method to determine the newly defined open field d-axis subtransient reactance x''_{do} . No extra test is needed to determine the q-circuit parameters. All three methods gave close results in laboratory tests.

A new multi-machine state variable formulation is presented in Chapter 3. The largest matrix inversion is the nodal admittance matrix Y_N . All system parameters are retained in the final formulation, convenient for sensitivity studies. Systems with an infinite bus are also considered. The results have the same form as that of multi-machine systems without an infinite bus. Dynamic simplification of power systems is discussed. It is found from a numerical example that conventional simplification in power system engineering retains the most dominant eigenvalues of the system.

A new technique for the design of optimal linear regulators is developed in Chapter 4. The weighting matrix Q of the regulator performance function is determined in conjunction with the dominant eigenvalue shift of the closed loop system. The eigenvalue sensitivities of the optimal closed loop system with respect to the Q elements are expressed in terms of the same eigenvector matrix of the composite matrix

M of equation (4.18), which is required for computing the Riccati matrix K.

Applying the technique developed in Chapter 4, the optimal stabilization of a one machine infinite system is investigated in Chapter 5. Three different methods of stabilization are considered, through excitation, through the governor, or through both as compared with the conventional stabilization through excitation control. It is found that optimal stabilization through excitation is more effective than conventional excitation stabilization, that optimal stabilization through a governor without dashpot is better than that through a governor with a dashpot, and that optimal stabilization through both excitation and governor without dashpot is the best of all.

In Chapter 6, the stabilization of multi-machine systems is investigated again using the technique developed in Chapter 4. Several cases are considered. It is found that a multi-machine system with multi-machine optimal controller u_{EM} , is better than the multi-machine system with only one optimal controller, u_{EI} , which is in turn better than the multi-machine system with the approximated one machine infinite system controller u_E . It is also found that although the individual optimal controller designs are effective in providing damping to individual machines, their effects on other machines are unpredictable. Therefore the dynamic coupling of the multi-machine system must always be included in optimal controller design.

The optimal controllers in Chapters 5 and 6 are all for nominal system operating conditions. Since the operating conditions of a real system change from time to time, the controllers so far designed are not adequate for varying operating conditions. In an attempt to face this

challenge an optimally sensitive controller is designed in Chapter 7. It is found that the newly developed optimally sensitive controller can adjust itself to stabilize a power system over a wide range of operating conditions and the optimum stabilization is always achieved. A new method to solve the Lyapunov type matrix equation necessary for the design is also developed.

Although the techniques have been tested on the detailed nonlinear mathematical model of the systems, it is highly desirable to implement them on a real power system. Other problems remain to be solved. One is to develop test methods to determine exact parameters of synchronous machines with additional rotor circuits. Another problem is how to obtain better approximate representation for system loads and infinite systems for power system dynamic studies. Finally there is the challenging problem of nonlinear optimal stabilization, which needs more investigation to make it practical.

APPENDIX A

MULTI-MACHINE STATE FORM EQUATIONS
FOR 5th ORDER SYNCHRONOUS MACHINE MODEL

For a 5th order synchronous machine model, the damper flux linkage variations are neglected, i.e.

$$p\Delta\psi_D = 0, \quad (\text{A.1})$$

$$p\Delta\psi_Q = 0, \quad (\text{A.2})$$

implementing (A.1) and (A.2) into (3.30) and eliminating $\Delta\psi_D$ and $\Delta\psi_Q$ from the results, system equations become,

$$\dot{Y} = AY + Bu, \quad (\text{A.3})$$

$$Y = \Delta(\psi_F \ \psi_d \ \psi_q \ v_F \ v_R \ \delta \ \omega_e)', \quad (\text{A.3a})$$

$$u = u_E, \quad (\text{A.3b})$$

$$B = [0 \ 0 \ 0 \ 0 \ \frac{K_A}{T_A} \ 0 \ 0]', \quad (\text{A.3c})$$

$$A = \begin{bmatrix} -r_F Y'_{FF} & -r_F Y'_{Fd} & 0 & I & 0 & 0 & 0 \\ -RY'_{dF} & -RY'_{dd} & \omega_e + X_m Y'_{qq} & 0 & 0 & -U_{mq} & [\psi_q] \\ -X_m Y'_{dF} & -\omega_e - X_m Y'_{dd} & -RY'_{qq} & 0 & 0 & U_{md} & -[\psi_d] \\ 0 & 0 & 0 & \frac{-1}{T_E} & \frac{1}{T_E} & 0 & 0 \\ MY'_{dF} & MY'_{dd} & NY'_{qq} & 0 & \frac{-1}{T_A} & A(5,6) & 0 \\ 0 & 0 & 0 & 0 & 0 & 0 & I \\ A(7,1) & A(7,2) & A(7,3) & 0 & 0 & 0 & \frac{-\omega_e t}{2H} D \end{bmatrix} \quad (\text{A.3d})$$

where

$$A(5,6) = \left[\frac{K_A}{T_A v_t} \right] (V_d U_{mq} - V_q U_{md})$$

$$A(7,1) = - \frac{\omega_o^2}{2H} \psi_q Y'_{dF}$$

$$A(7,2) = - \frac{\omega_o^2}{2H} \psi_q (Y'_{dd} - Y'_{qq})$$

$$A(7,3) = - \frac{\omega_o^2}{2H} \{ \psi_d (Y'_{dd} - Y'_{qq}) + \psi_F Y'_{dF} \}$$

$$Y'_{FF} = Y_{FF} - Y_{FD} Y_{DD}^{-1} \quad Y_{DF} = \omega_o x_d / x_F x'_d$$

$$Y'_{dF} = Y_{dF} - Y_{dD} Y_{DD}^{-1} \quad Y_{DF} = - \omega_o x_{dF} / x_F x'_d \quad (A.3e)$$

$$Y'_{Fd} = Y_{Fd} - Y_{FD} Y_{DD}^{-1} \quad Y_{Dd} = - \omega_o x_{Fd} / x_F x'_d$$

$$Y'_{dd} = Y_{dd} - Y_{dD} Y_{DD}^{-1} \quad Y_{Dd} = \omega_o / x'_d$$

$$Y'_{qq} = Y_{qq} - Y_{qQ} Y_{QQ}^{-1} \quad Y_{Qq} = \omega_o / x_q$$

M and N are as given in (3.21a). The governor equations can be easily incorporated into (A.3) if required.

APPENDIX B

FREQUENCY DOMAIN SOLUTION OF LYAPUNOV MATRIX EQUATION

A new method for solving the Lyapunov matrix equation in the frequency domain is proposed. The highest matrix order used in the computation is the same as the system matrix and no matrix inversion is required. Two algorithms are given, the first uses the Leverrier algorithm and the second uses the eigensystem of the system matrix. The equation is usually of the form

$$A^T K + KA = -Q \quad (B.1)$$

where A is the system matrix, K the matrix to be solved and Q a positive semi-definite symmetric matrix. Equation (B.1) consists of essentially $n(n+1)/2$ linear equations for an n-order system. The equation can be expanded as

$$N^k = q \quad (B.2)$$

and solved directly. Since for a stable system

$$K = \int_0^{\infty} e^{A^T t} Q e^{At} dt \quad (B.3)$$

which has finite value, the integral can be approximated as a series summation and evaluated iteratively^{38,39}. Transformation approaches are also reported^{40,41,42}. Solutions are obtained after (B.1) is reduced to a special form.

In what follows, the method of frequency domain solution of (B.1) will be presented. Applying Parseval's theorem (B.3) becomes

$$K = \frac{1}{2\pi j} \int_{-j\infty}^{j\infty} F(s) ds \quad (B.4)$$

where

$$F(s) = (-sI - A^T)^{-1} Q(sI - A)^{-1} \quad (B.5)$$

K can thus be evaluated from the residue theorem. Let

$$(sI - A)^{-1} = R(s)/g(s) \quad (B.6)$$

where

$$\begin{aligned} R(s) &= Is^{n-1} + R_1s^{n-2} + \dots + R_1s^{n-i-1} + \dots + R_{n-1} \\ g(s) &= \det(sI - A) = s^n - h_1s^{n-1} - \dots - h_1s^{n-i} - \dots - h_n \\ & \quad i = 1, 2, \dots, n \end{aligned} \quad (B.7)$$

The matrix coefficients R_i of the adjoint matrix polynomial $R(s)$ and the scalar coefficients h_i of the characteristic equation $g(s)$ can be determined simultaneously by Leverrier's algorithm³³,

$$\begin{aligned} h_i &= \frac{1}{i} \text{trace } [A_i], \quad R_i = A_i - h_i I \\ A_1 &= A, \quad A_i = AR_{i-1} \end{aligned} \quad (B.8)$$

substituting (B.6) into (B.5) gives

$$F(s) = \frac{R^T(-s)}{g(-s)} Q \frac{R(s)}{g(s)} \quad (B.9)$$

which can be written as

$$F(s) = \sum_{i=1}^n \frac{C_i}{s-\lambda_i} + \sum_{i=1}^n \frac{D_i}{s+\lambda_i} \quad (B.10)$$

where C_i and D_i are residue matrices of $F(s)$ in the left and right half complex planes respectively. It is assumed that λ_i are distinct. Let $g'(s) = d \cdot g(s)/ds$. Then

$$C_i = (s - \lambda_i) \cdot F(s) \Big|_{s=\lambda_i} = \frac{R^T(-\lambda_i)}{g(-\lambda_i)} Q \frac{R(\lambda_i)}{g'(\lambda_i)} \quad (\text{B.11})$$

or

$$C_i = - \frac{R^T(-\lambda_i) Q R(\lambda_i)}{2\lambda_i \prod_{j \neq i} (\lambda_j^2 - \lambda_i^2)} \quad (\text{B.12})$$

Applying the residue theorem one has

$$K = \sum_{i=1}^n C_i \quad (\text{B.13})$$

Since

$$C_{i+1} = C_i^* \quad (\text{B.14})$$

for conjugate-pair roots, $\lambda_{i+1} = \lambda_i^*$. For a system with m conjugate pair roots and l real roots,

$$K = 2 \sum_{i=1}^m \text{Real } C_{2i-1} + \sum_{j=2m+1}^n C_j \quad (\text{B.15})$$

The residue matrices C_i can be computed also from the eigenvalues and eigenvectors of the system. Since

$$\frac{R(s)}{g(s)} = \sum_{j=1}^n \frac{R(\lambda_j)}{g'(\lambda_j)(s-\lambda_j)} \quad (\text{B.16})$$

and Morgan has shown that⁴³

$$x_j v_j^T = \frac{R(\lambda_j)}{g'(\lambda_j)} \quad (\text{B.17})$$

where x_j and v_j are the normalized j -th eigenvectors of A and A^T respectively, equation (11) may be written as

$$\begin{aligned} C_i &= \sum_{j=1}^n \frac{R^T(\lambda_j)}{g'(\lambda_j)(-\lambda_i - \lambda_j)} Q \frac{R(\lambda_i)}{g'(\lambda_i)} \\ &= - \sum_{j=1}^n \frac{v_j x_j^T}{\lambda_j + \lambda_i} Q x_i v_i^T \end{aligned}$$

$$= -V\Lambda_i X_i^T Q x_i v_i^T \quad (\text{B.18})$$

where

$$\Lambda_i = \text{diag}[\lambda_i + \lambda_1, \lambda_i + \lambda_2, \dots, \lambda_i + \lambda_n] \quad (\text{B.19})$$

and X, V are eigenvector matrices of columns of x_i and v_i , respectively;

$i = 1, \dots, n.$

REFERENCES

1. H.M. Ellis, J.E. Hardy, A.L. Blythe and J.W. Skooglund, "Dynamic Stability of the Peace River System", IEEE Transactions, Vol. PAS-85, pp. 586-600, June 1966.
2. P.L. Dandeno, A.N. Karas, K.R. McClymont and W. Watson, "Effect of High-Speed Rectifier Excitation Systems on Generator Stability Limits", IEEE Transactions, Vol. PAS-87, pp. 190-201, January 1968.
3. O.W. Hanson, C.J. Goodwin, and P.L. Dandeno, "Influence of Excitation and Speed Control Parameters in Stabilizing Intersystem Oscillations", IEEE Transactions, Vol. PAS-87, pp. 1306-1313, May 1968.
4. F.R. Schleif, G.E. Martin, and R.R. Angell, "Damping of System Oscillations with a Hydrogenerating Unit", IEEE Transactions, Vol. PAS-86, pp. 438-442, April 1967.
5. F.R. Schleif, H.D. Humlins, G.E. Martin, and E.E. Hattan, "Excitation Control to Improve Powerline Stability", IEEE Transactions, Vol. PAS-87, pp. 1426-1434, June 1968.
6. F.R. Schleif, H.D. Hunkins, E.E. Hattan, and W.B. Gish, "Control of Rotating Exciters for Power System Damping-Pilot Applications and Experience", IEEE Transactions, Vol. PAS-88, pp. 1259-1266, August 1969.
7. R.M. Shier, and A.L. Blythe, "Field Tests of Dynamic Stability Using a Stabilizing Signal and Computer Program Verification", IEEE Transactions, Vol. PAS-87, pp. 315-322, February 1968.
8. R.T. Byerly, F.W. Keay, and J.W. Skooglund, "Damping of Power Oscillations in Salient Pole Machines With Static Exciters", IEEE Transactions, Vol. PAS-89, pp. 1009-1021, July/August 1970

9. F.P. deMello and C. Concordia, "Concepts of Synchronous Machine Stability as Affected by Excitation Control", IEEE Transactions, Vol. PAS-88, pp. 316-329, April 1969.
10. P.C. Krause and J.N. Towle, "Synchronous Machine Damping by Excitation Control with Direct and Quadrature Axis Field Windings", IEEE Transactions, Vol. PAS-88, pp. 1266-1274, August 1969.
11. Y.N. Yu, K. Vongsuriya, and L.N. Wedman, "Application of an Optimal Control Theory to a Power System", IEEE Transactions, Vol. PAS-89, pp. 55-62, January 1970.
12. Y.N. Yu and C. Siggers, "Stabilization and Optimal Control Signals for a Power System", presented at IEEE Summer Power Meeting, paper No. 70TP531-PWR.
13. Yao-nan Yu and H.A.M. Moussa, "Experimental Determination of Exact Equivalent Circuit Parameters of Synchronous Machines", 1971 IEEE Winter Power Meeting, paper No. 71 TP 63-PWR.
14. I.M. Canay, "Causes of Discrepancies on Calculation of Rotor Quantities and Exact Equivalent Diagrams of the Synchronous Machine." IEEE Transactions, PAS-88 No. 7, July 1969, pp. 1114-1120.
15. C. Concordia, "Synchronous Machines" (book), John Wiley, 1951, eqts. (21) and (24), pp. 14-15.
16. A.W. Rankin, "Per-unit Impedances of Synchronous Machines,"
 - I. AIEE T. Vol. 64 pp. 569-573, 1945
 - II. AIEE T. Vol. 64 pp. 839-841, 1945.
17. "Test Procedure for Synchronous Machines," IEEE Publ. 115, 1965.
18. B. Adkins, "The General Theory of Electrical Machines," (book), Chapman and Hall 1964, pp. 122-123.

19. H. Kaminosono and K. Uyeda, "New Measurement of Synchronous Machine Quantities," IEEE Transactions, PAS-87, No. 11, Nov. 1968, pp. 1908-1918.
20. F.K. Dalton and A.W. Cameron, "Simplified Measurement of Subtransient and Negative Sequence Reactances in Salient-pole Synchronous Machines," AIEE Trans., PAS-71, pp. 752-757, Oct. 1952.
21. Yao-nan Yu and H.A.M. Moussa, "Optimal Stabilization of a Multi-Machine System", 1971 IEEE Summer Power Meeting, paper No. 71 CP 603-PWR.
22. W.A. Laughton, "Matrix Analysis of Dynamic Stability in Synchronous Multi-machine Systems", Proc. IEE, Vol. 113, No. 2, pp. 325-336, Feb. 1966.
23. John M. Undrill, "Dynamic Stability Calculations for an Arbitrary Number of Interconnected Synchronous Machines", IEEE Transactions, Vol. PAS-87, pp. 835-844, March 1968.
24. John M. Undrill, "Structure in the Computation of Power-System Nonlinear Dynamical Response", IEEE Transactions, Vol. PAS-88, pp. 1-6, Jan. 1969.
25. E.J. Davison, "A Method for Simplifying Linear Dynamic Systems", IEEE Transactions on Automatic Control, Vol. AC-11, pp. 93-101, January 1966.
E.J. Davison, "A New Method for Simplifying Linear Dynamic Systems", Ibid, Vol. AC-13, pp. 214-215, April 1968.
26. M.R. Chidambara, "Two Simple Techniques For the Simplification of Large Dynamic Systems", Preprints, 1969 JACC, pp. 669-674.
27. H.A.M. Moussa and Yao-nan Yu, "Optimal Power System Stabilization Through Excitation and/or Governor Control", 1971 IEEE Summer Power Meeting, paper No. 71 TP 581-PWR.

28. C.E. Fosha Jr., and O.I. Elgerd, "The Megawatt-Frequency Control Problem: A New Approach via Optimal Control Theory", IEEE Transactions, Vol. PAS-89, pp. 563-577, April 1970.
29. M. Athans, and P.L. Falb, "Optimal Control", (book), McGraw Hill, New York, 1966.
30. Robert T.N. Chen and David W.C. Shen, "Sensitivity Analysis and Design of Multivariable Regulators using a Quadratic Performance Criterion", Preprints, 1968 JACC, pp. 229-238.
31. James E. Potter, "Matrix Quadratic Solutions", SIAM, Journal of Applied Math, Vol. 14, No. 3, pp. 496-506, May 1966.
32. C.E. Fosha Jr. and O.I. Elgerd, "Optimum Linear Control of the Multi-variable Megawatt-Frequency Control Problem", Preprints, 1969 JACC, pp. 471-472.
33. D.K. Faddeev and V.N. Faddeeva, "Computational Methods of Linear Algebra", (book), Freeman, 1963.
34. Hamdy A.M. Moussa, and Yao-nan Yu, "Optimum Stabilization of Power Systems Over Wide Range Operating Conditions" Submitted to 1972 IEEE Winter Power Meeting.
35. H.J. Kelley, "An Optimal Guidance Approximation Theory", IEEE Transactions on Automatic Control, Vol. AC-9, pp. 375-380, October 1964.
36. R.A. Werner, and J.B. Cruz, Jr., "Feedback Control Which Preserves Optimality for Systems with Unknown Parameters" IEEE Transactions on Automatic Control, Vol. AC-13, pp. 621-629, December 1968.

37. P.V. Kokotovic, J.B. Cruz, Jr., J.E. Heller, and P. Sannuti, "Synthesis of Optimally Sensitive Systems", Proceedings of the IEEE, Vol. 56, pp. 1318-1324, August 1968.
38. Davison, E.J. and Man, F.T.: "The Numerical Solution of $A'Q+QA = -C$ ", IEEE Trans., 1968, AC-13, pp. 448-449.
39. Wedman, L.N. and Yu, Y.N.: "Computation Techniques for the Stabilization and Optimization of High Order Systems", IEEE PICA Conference Proc., 1969, pp. 324-343.
40. Barnett, S. and Storey, C.: "Stability Analysis of Constant Linear Systems by Lyapunov's Second Method", Electron. Lett., 1966, 2, pp. 165-166.
41. Power, H.M.: "Further Comments on the Lyapunov Matrix Equation", Electron. Lett., 1967, 3, pp. 153-154.
42. Molinari, B.P.: "Algebraic Solution of Matrix Linear Equations in Control Theory", Proc. IEE, 1969, 116-10, pp. 1748-1754.
43. Morgan, B.S., "Computational Procedure for Sensitivity of an Eigenvalue", Electron. Lett., 1966, 2, pp. 197-198.